To the Graduate Council:

I am submitting herewith a thesis written by Brian L. Myruski entitled "SSME Nozzle Flow Field Calculations Using Equilibrium PARC Code." I have examined the final copy of this thesis for form and content and recommend that it be accepted in partial fulfillment of the requirements for the degree of Master of Science, with a major in Mechanical Engineering.

Frank G. Collins

Frank G. Collins, Major Professor

We have read this thesis
and recommend its acceptance:

George W Garrison

Charles C. Limbaugh

Accepted for the Council:

Lew Minkel

Vice Provost
and Dean of the Graduate School

STATEMENT OF PERMISSION TO USE

In presenting this dissertation in partial fulfillment of the requirements for a Master's degree at The University of Tennessee, Knoxville, I agree that the Library shall make it available to borrowers under rules of the Library. Brief quotations from this thesis are allowable without special permission, provided that accurate acknowledgment of the source is made.

Permission for extensive quotation from or reproduction of this thesis may be granted by my major professor, or in his absence, by the Head of Interlibrary Services when, in the opinion of either, the proposed use of the material is for scholarly purposes. Any copying or use of the material in this thesis for financial gain shall not be allowed without my written permission.

Signature Brian Myers

Date August 1990

SSME NOZZLE FLOW FIELD CALCULATIONS USING EQUILIBRIUM PARC CODE

A Thesis

Presented for the

Master of Science

Degree

The University of Tennessee, Knoxville

Brian L. Myruski

December 1990

ABSTRACT

The purpose of this research was to enhance the PARC Navier-Stokes computer code by adding hydrogen-oxygen equilibrium chemistry as an option when solving chemically reacting flow problems.

Modifications to the PARC code were made by combining classical thermodynamics, statistical thermodynamics, and kinetic theory calculations to calculate the equilibrium and transport properties of the flow.

The new equilibrium version of the code was then used to calculate the SSME nozzle flow field and the results were compared with the constant specific heat solution. As expected, higher nozzle performance was predicted due to increased energy release by the equilibrium flow. Nozzle performance parameters also compared very well with results from the NASA Two-Dimensional Kinetic code (TDK) and the measured test data.

TABLE OF CONTENTS

CHAPTER		PAGE
I.	INTRODUCTION	1
II.	DESCRIPTION OF THE PARC CODE	4
III.	CHEMICAL EQUILIBRIUM MODEL	6
	Statistical Mechanics Calculations	8
	Equilibrium Calculations	9
	Transport Property Calculations	19
	Adiabatic Flame Temperature	19
	The Varible Beta (β)	23
	Performance Calculations	24
	Added Convergence Parameters	26
IV.	COMPUTATIONS ON THE SSME NOZZLE	28
	Assumptions	28
	Grid	28
	Convergence Procedure	28
	Results and Comparisons	29
V.	SUMMARY AND CONCLUSIONS	52
	LIST OF REFERENCES	54
	APPENDICES	58
	A. PARTITION FUNCTIONS AND SPECTROSCOPIC CONSTANTS	59
	B. EQUILIBRIUM CONSTANTS	69
	C. EQUILIBRIUM COMPOSITION NEWTON-RAPHSON EQUATIONS	70
	D. PARTIAL DERIVATIVES OF THE EQUILIBRIUM CONSTANT	75

CHAPTER PAGE

E. TRANSPORT PROPERTY EQUATIONS 78

F. METHOD OF BISECTION 81

G. EQUATIONS FOR NONDIMENSIONALIZATION OF PARC . . . 82

VITA 84

LIST OF FIGURES

FIGURE		PAGE
1.	Equilibrium Composition at 1 Atm, O/F = 6.0	12
2.	Constant Pressure Specific Heat, C_p	16
3.	Equilibrium Gamma, O/F = 6.0	17
4.	Mixture Molecular Weight, O/F = 6.0	18
5.	Mixture Viscosity, O/F = 6.0	20
6.	Thermal Conductivity, O/F = 6.0	21
7.	Beta (Ratio of Enthalpy to Internal Energy) versus Temperature	25
8.	Mach Number Contour Comparison	31
9.	Series of Expansion and Compression Waves Inside a Nozzle with an Internal Shock	32
10.	Mach Contour from [17] Axial Gamma Variation, Coarse Grid	33
11.	SSME Molecular Weight Contour	34
12.	SSME Temperature Along Centerline, Equilibrium	35
13.	SSME Mach Number Along Centerline, Equilibrium	36
14.	SSME Equilibrium Gamma Along Centerline	37
15.	SSME Molecular Weight Along Centerline, Equilibrium	38
16.	Comparison of Exit Velocities	39
17.	Temperature Comparison Along Centerline	41
18.	Centerline Axial Velocity Comparison	42
19.	Velocity Profiles in Boundary Layer, Exit Plane	45
20.	Temperature Profile in Boundary Layer, Exit Plane	46

FIGURE PAGE

21. Normalized Velocity Profile in Boundary Layer, Exit Plane 47

22. Normalized Temperature Profiles in Boundary Layer, Exit Plane 48

23. Equilibrium Gamma Across the Boundary Layer, Exit Plane . . 49

24. Molecular Weight Across the Boundary Layer, Exit Plane . . 50

NOMENCLATURE

A	Area
a	Speed of sound
B_e	Constant relating to moment of inertia
c	Speed of light
$\dot{C}_1, \dot{C}_2, C_1, C_2$	Designated terms in Newton-Raphson equilibrium equations
C	Mass fraction
C_p	Constant pressure specific heat
C_v	Constant volume specific heat
D_e	Spectroscopic heat of dissociation
e	Internal energy
F	Thrust
$f, O/F$	Oxygen/hydrogen fuel weight ratio
g	Degeneracy
g_e	Acceleration of gravity at earth's surface
$\bar{h}_f^o$	Enthalpy of formation
Δh	Change in enthalpy from the reference state
H, h	Enthalpy
h	Planck's constant
I_x, I_y, I_z	Product of moments of inertia
I_{sp}	Specific impulse
k	Thermal conductivity Boltzman's constant
K	Equilibrium constant as a function of temperature
K'	Equilibrium constant as a function of temperature and pressure

$\dot{K}'$	Partial derivative of K' with respect to temperature
M	Mach number
m	Mass
$\dot{m}$	Mass flow
P	Pressure
po	Standard state pressure, 1 atm
q	Partition function
r_e	Equilibrium separation distance
R	Specific gas constant
$\bar{R}$	Universal gas constant
T_e	Characteristic temperature
T	Temperature
u_e, u_v, y	Spectroscopic constants defined in Appendix A
V	Velocity
v	Stoicometric coefficient
w_e	Classical vibration frequency
w	Temperature relaxation variable
W	Molecular weight
X_e	Anharmonicity constant
X	Mole fraction
$\dot{X}$	Partial derivative of mole fraction with respect to temperature
α_e	Correction due to changing moment of inertia due to the vibration associated with rotation
β	Ratio of enthalpy to internal energy
γ	Ratio of specific heats

σ	Symmetry number
ρ	Density
η	Number of moles
η_T	Total number of moles
μ	Viscosity
θ_v	Characteristic temperature for vibration
θ_D	Characteristic temperature for dissociation
θ_i	Characteristic temperature for electronic level i

SUBSCRIPTS

tot	Total
tr	Transitional
rot	Rotational
vib	Vibrational
corr	Correctional
elec	Electronic
i,j,k,ℓ	Denote species
j	Denotes reaction

CHAPTER I

INTRODUCTION

The nozzles for future space engines will incorporate many features that cannot be handled adequately by existing performance prediction techniques such as the Joint Army, Navy, NASA, Air Force (JANNAF) methodology utilized in the Two-Dimensional Kinetics Computer Program (TDK) code [1].[1] Future nozzles could have higher area ratios and lower operating pressures, leading to thick boundary layers and possibly rarefaction effects at the exit. Some could also have novel wall contouring, novel wall cooling, and/or variable geometry. One main disadvantage of the TDK code is the uncoupled nature of the calculations, which means that the core flow and boundary layer are computed separately and in an iterative procedure, the solution of the core flow is incorporated into the boundary layer calculations and vice-versa. This is adequate for flows with thin boundary layers but as the boundary layer thickens, viscous/inviscid interactions errors become more prominent.

The PAR2D Navier-Stokes code [2] was developed by Sverdrup Technology, Inc. at the Arnold Engineering Development Center (AEDC). One major advantage it has over the TDK Code is that the boundary layer and core flow are solved simultaneously so it is better able to calculate flows with thick boundary layers. Other advantages include greater

---

[1]Letters in brackets refer to similarly numbered references in the List of References.

flexibility in the kinds of boundary conditions and geometries which can be used.

The present work is part of a multi-phase effort between the Center for Advanced Space Propulsion (CASP) and Rocketdyne Division, Rockwell International Corporation to enhance the PARC2D code for use in designing advanced space engine nozzles. Specifically this thesis deals with the development of hydrogen-oxygen equilibrium chemistry into the PARC2D calculations. Although equilibrium chemistry is certainly not a true model of actual chemistry, when results of equilibrium flow analysis are used in context with test data or other computations such as "frozen" chemistry, they provide useful insights into the physical nature of the actual flow.

The present work was preceded by that of Orr [3], who worked extensively with the original (perfect gas) PARC code in applications to rocket nozzles, and Salidino [4], who developed an equilibrium air chemistry option for PARC2D. Much of the work involved in the hydrogen-oxygen equilibrium project was modification of the equilibrium air PARC code.

The equilibrium PARC code was used to compute the flow field of the Space Shuttle Main Engine (SSME) rocket nozzle. The equilibrium PARC solution was compared to the measured test data, the TDK code, another Navier-Stokes solution, and the previous work of Orr. The equilibrium PARC code calculations were done assuming an adiabatic wall, 3000 psia chamber pressure, and an oxygen-hydrogen fuel weight ratio (O/F) of 6.0. A laminar boundary layer was assumed because

these calculations generally proceed much easier than turbulent calculations. This is important for the first running of the code. Also, the importance of the turbulent boundary layer is best judged by comparison to the laminar boundary layer. Future turbulent boundary layer equilibrium PARC code calculations are planned.

CHAPTER II

DESCRIPTION OF THE PARC CODE

The PARC code is a flow field simulation program which calculates the thermodynamic and kinematic properties of a fluid flow at discrete points within the flow based on specified boundary conditions and geometry. PARC has both two-dimensional (PAR2D) and three-dimensional (PAR3D) versions. Inviscid and viscous flows can be calculated. Viscous flows can be laminar or turbulent and can be treated as fully viscous or shear-layer flows.

The basis of the algorithms in PARC is the complete Navier-Stokes equations in conservation law form. This is the divergence form of the time-dependent continuity, momentum, and energy equations. Although the code has been used to solve transient flow problems, it is primarily designed to solve steady-state problems using the unsteady formulation of the Navier-Stokes equations only as a means to construct an iterative solution algorithm. Spatial or temporal time steps can be selected to achieve the maximum convergence rate.

The major features of PARC are summarized in Table 1. For more information the reader should refer to [2] and [5].

Table 1. Features of PARC Computational Code [6]

- Uses full viscous, compressible Navier-Stokes equations written in strong conservative form for shock capturing;
- Uses the Beam-Warming appropriate factorization algorithm [7] and Pulliam's scalar pentadiagonal transformation to produce a steady-state solver [8,9];
- Gamma, gas composition and Prandtl number are constant and Stokes hypothesis is assumed; Sutherland transport model is used;
- Jameson-type artificial viscosity formulation [10] is applied as a function of coordinate direction, and is limited by the local cell Reynolds number;
- P.D. Thomas formation of Baldwin-Lomax algebraic turbulence models [11], [12], and K-ε turbulence model are available [13];
- Incorporates general boundary conditions which are input to the code;
- Contains flexible time-step control, involving both spatial and temporally varying time-steps, allowing maximum convergence rate.

CHAPTER III

CHEMICAL EQUILIBRIUM MODEL

The original PARC code considers the fluid to be a calorically perfect gas. A calorically perfect gas has constant specific heats (C_p and C_v) and obeys the perfect gas equation of state given by:

$$P = \rho RT = \rho \frac{\overline{R}}{W} T$$

where $\overline{R}$ = universal gas constant,

W = molecular weight

P = pressure,

T = temperature,

ρ = density.

The equilibrium chemistry modification considers the fluid to be a chemically reacting mixture of thermally perfect gasses in chemical and thermal equilibrium. This is a mixture of individual species which obey the perfect gas law but are not calorically perfect because their individual specific heats vary with temperature. Equilibrium can be thought of as that state in which the individual species of the fluid react with each other so that at any particular thermodynamic state, the composition is determined by the minimization of the free energy of the system. In a flow system, chemical equilibrium requires that reaction rates occur much faster than the changes in temperature and pressure which are encountered by the flow. Chemically reacting mixtures in equilibrium are discussed in detail in both [14] and [15].

The chemically reacting mixture in the SSME rocket nozzle comes from the combustion of hydrogen and oxygen. The following reactions are used to model the equilibrium mixture.

1) $H_2 \rightleftharpoons 2H$

2) $O_2 \rightleftharpoons 2O$

3) $OH \rightleftharpoons O+H$

4) $H_2O \rightleftharpoons 2H+O$

5) $HO_2 \rightleftharpoons H+2O$

These equations were deemed adequate in describing the mixture composition by examining the equilibirum composition as calculated by the code described in NASA-SP-273 [16]. The judgement was based upon a solution to a larger system of reaction equations over the expected temperature ranges. Species with mole fractions less than 0.00004 were considered to be trace and were eliminated from the system. This left only the species listed in the above reactions.

The calculation of the composition and properties is separated into three basic sections designated as the statistical mechanics, equilibrium and transport property calculations. The statistical mechanics section calculates the thermodynamic properties of each individual species in the mixture and the equilibrium constants used in the equilibrium section. The equilibrium section calculates the equilibrium composition and the thermodynamic properties of the mixture. The transport property section calculates the viscosity and thermal conductivity of the equilibrium mixture. Other modifications for the operation of the equilibrium PARC Code include the following:

1) Adiabatic flame temperature is calculated for use as stagnation temperature.
2) The reference state for enthalpy and internal energy was changed in the fluid-dynamics solver (the original PARC code) through the variable β.
3) The performance parameters of mass flow, thrust, and specific impulse are calculated.
4) Two variables (NXPRT and w) were added to help maximize the convergence rate.

The following sections describe the calculations and modifications in more detail.

Statistical Mechanics Calculations

In this section of calculations, the enthalpy and constant pressure specific heat are calculated for each species in the equilibrium mixture at the specified nodal temperature and pressure. This section also calculates the equilibrium constants (described in the Equilibrium Calculations section) for the five reaction equations considered. The properties and equilibrium constants are calculated using a quantum and statistical mechanics approach described in [4] and [17].

Appendix A lists the equations used in calculating enthalpy and specific heat and the spectroscopic constants for each species. Appendix B lists the equations for the equilibrium constants.

Equilibrium Calculations

The equilibrium section calculates the composition and thermodynamic properties of the mixture from the properties and constants calculated in the statistical mechanics section.

The basic equations used in the calculation of the equilibrium compositions are derived in [14] using the minimization of Gibb's free energy principles. For the reaction

$$\nu_A A + \nu_B B \rightleftharpoons \nu_C C + \nu_D D$$

where ν_i = Stoichometic coefficients of the reaction, the equilibrium constant is given by

$$K = \frac{X_A^{\nu_A} X_B^{\nu_B}}{X_C^{\nu_C} X_D^{\nu_D}} \left(\frac{P}{P^o}\right)^{\nu_C+\nu_D-\nu_A-\nu_B}$$

where X_A = mole fraction of species A

P^o = standard state pressure

This equilibrium constant is a function of temperature only. For convenience in solving for the composition, another equilibrium constant (K') is defined as

$$K' = \frac{X_A^{\nu_A} X_B^{\nu_B}}{X_C^{\nu_C} X_D^{\nu_D}} = \frac{K}{\left(\frac{P}{P^o}\right)^{\nu_C+\nu_D-\nu_A-\nu_B}}$$

Since the equilibrium constants for the five reactions of the equilibrium mixture are known from the statistical mechanics routine, it is possible to solve the system of non-linear equations for the equilibrium composition. The non-linear equations for this system become:

1) $$X_H^2 - K_1' X_{H_2} = 0$$

2) $$X_o^2 - K_2' X_{O_2} = 0$$

3) $$X_H X_o - K_3' X_{OH} = 0$$

4) $$X_H^2 X_o - K_4' X_{H_2O} = 0$$

5) $$X_H X_o^2 - K_5' X_{HO_2} = 0$$

6) $$X_H + X_o + X_{H_2} + X_{O_2} + X_{OH} + X_{H_2O} + X_{HO_2} - 1 = 0$$

7) $$\frac{C_1}{.126\,(f)} - \frac{C_2}{2} = 0$$

where,

$$C_1 = X_O + 2X_{O_2} + X_{OH} + X_{H_2O} + 2X_{HO_2}$$

$$C_2 = X_H + 2X_{H_2} + X_{OH} + 2X_{H_2O} + X_{HO_2}$$

$f = O/F = oxygen/hydrogen\ fuel\ weight\ ratio.$

A Newton-Raphson technique is used to solve these equations which are derived in Appendix C.

Sample results for composition versus temperature at 1 atm, and O/F of 6, are shown in Figure 1.

The equilibrium section also calculates the thermodynamic properties of the mixture. The equations for the equilibrium specific heats, C_p and C_v, are derived in [15].

$$C_p = \sum_i C_i C_{p_i} + \sum_i h_i \left(\frac{\partial C_i}{\partial T} \right)_P$$

$$C_v = \sum_i C_i C_{v_i} + \sum_i e_i \left(\frac{\partial C_i}{\partial T} \right)_\rho$$

where,

C_i = Mass Fraction

h_i = Enthalpy

e_i = Internal Energy

i denotes species.

C_{p_i} and h_i are calculated in the statistical mechanics routine. C_{v_i} and e_i are calculated from the perfect gas equations for the species as follows:

$$C_{v_i} = C_{P_i} - R$$

$$e_i = h_i - RT$$

where

$$R = \frac{\overline{R}}{W}$$

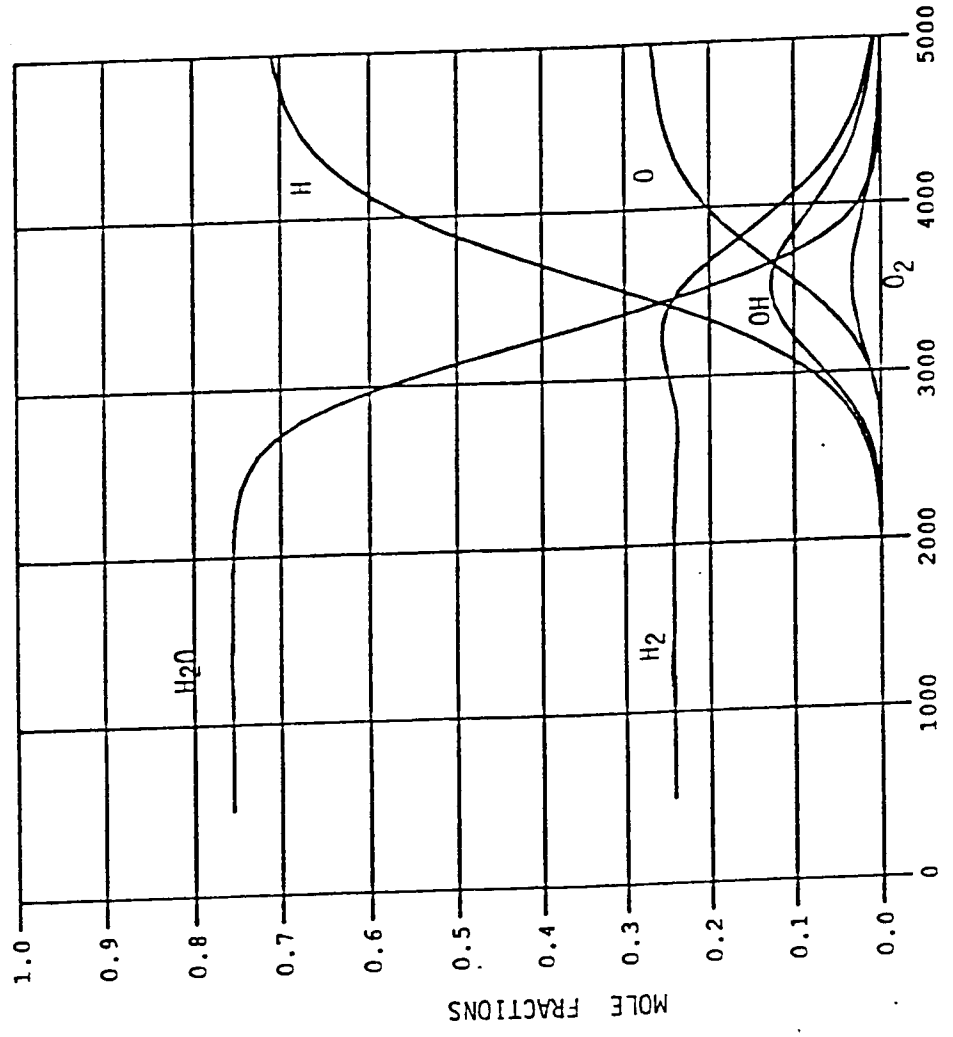


Figure 1. Equilibrium Composition at 1 Atm, O/F = 6.0

The mass fraction, C_i, is calculated from the equation

$$C_i = \frac{X_i W_i}{W} = \frac{X_i W_i}{\sum_{i=1}^{n} X_i W_i}$$

where,

W_i = Species Molecular Weight

X_i = Species Mole Fraction

The partial derivative terms were found as follows:

$$\left.\frac{\partial C_i}{\partial T}\right|_P = \frac{W_i}{W^2}\left[W\left(\frac{\partial X_i}{\partial T}\right)_P - X_i\left(\frac{\partial W}{\partial T}\right)_P\right]$$

$$= \frac{W_i}{W}\left[\left(\frac{\partial X_i}{\partial T}\right)_P - \frac{X_i}{W}\left(\frac{\partial W}{\partial T}\right)_P\right]$$

Similarly, for constant density:

$$\left.\frac{\partial C_i}{\partial T}\right|_\rho = \frac{W_i}{W}\left[\left(\frac{\partial X_i}{\partial T}\right)_\rho - \frac{X_i}{W}\left(\frac{\partial W}{\partial T}\right)_\rho\right]$$

the term

$$\frac{\partial W}{\partial T} = \sum_{i=1}^{n} \frac{\partial X_i}{\partial T} W_i.$$

This leaves the term $\partial X_i/\partial T$ to be found.

If the non-linear equilibrium equations are differentiated with respect to temperature, and another set of non-linear equations are obtained, as follows:

1) $$2X_H \dot{X}_H - \dot{K}_1' X_{H_2} - K_1' \dot{X}_{H_2} = 0$$

2) $$2X_O \dot{X}_O - \dot{K}_2' X_{O_2} - K_2' \dot{X}_{O_2} = 0$$

3) $$\dot{X}_H X_O + \dot{X}_O X_H - \dot{K}_3' X_{OH} - K_3' \dot{X}_{OH} = 0$$

4) $$2X_H \dot{X}_H X_O + X_H^2 \dot{X}_O - \dot{K}_4' X_{H_2O} - K_4' \dot{X}_{H_2O} = 0$$

5) $$2X_O X_H \dot{X}_O + X_O^2 \dot{X}_H - \dot{K}_5' X_{HO_2} - K_5' \dot{X}_{HO_2} = 0$$

6) $$\dot{X}_H + \dot{X}_O + \dot{X}_{H_2} + \dot{X}_{O_2} + \dot{X}_{OH} + \dot{X}_{H_2O} + \dot{X}_{HO_2} = 0$$

7) $$\frac{\dot{C}_1}{.126\, f} - \frac{\dot{C}_2}{2} = 0$$

where

$$\dot{C}_1 = \dot{X}_O + 2\dot{X}_{O_2} + \dot{X}_{OH} + \dot{X}_{H_2O} + 2\dot{X}_{HO_2}$$

$$\dot{C}_2 = \dot{X}_H + 2\dot{X}_{H_2} + \dot{X}_{OH} + 2\dot{X}_{H_2O} + \dot{X}_{HO_2}$$

$$\dot{X}_i = \frac{\partial X_i}{\partial T}$$

$$\dot{K}_j' = \frac{\partial K_j'}{\partial T}$$

i denotes species,

j denotes the reaction.

If the K_j' are found, these equations can be solved for X_i using the Newton-Raphson method again. There is a K_j' for constant pressure and another for constant density. These are derived in Appendix D. Figure 2 is a graph of the equilibrium specific heat at constant pressure, C_p versus temperature at several pressures and a O/F of 6.0. Figure 3 is the ratio of the equilibrium specific heats ($\gamma = C_p/C_v$) versus temperatures for the same conditions as Figure 2.

The equilibrium mixture enthalpy, h, and internal energy, e, are calculated from:

$$h = \sum_i X_i h_i$$

$$e = \sum_i X_i e_i = \sum_i X_i \left(h_i - RT \right)$$

The equilibrium mixture molecular weight, W, which is calculated by

$$W = \sum_i X_i W_i$$

is shown versus temperature in Figure 4.

The results of this section were validated by comparison of the figures presented here and those presented in [18].

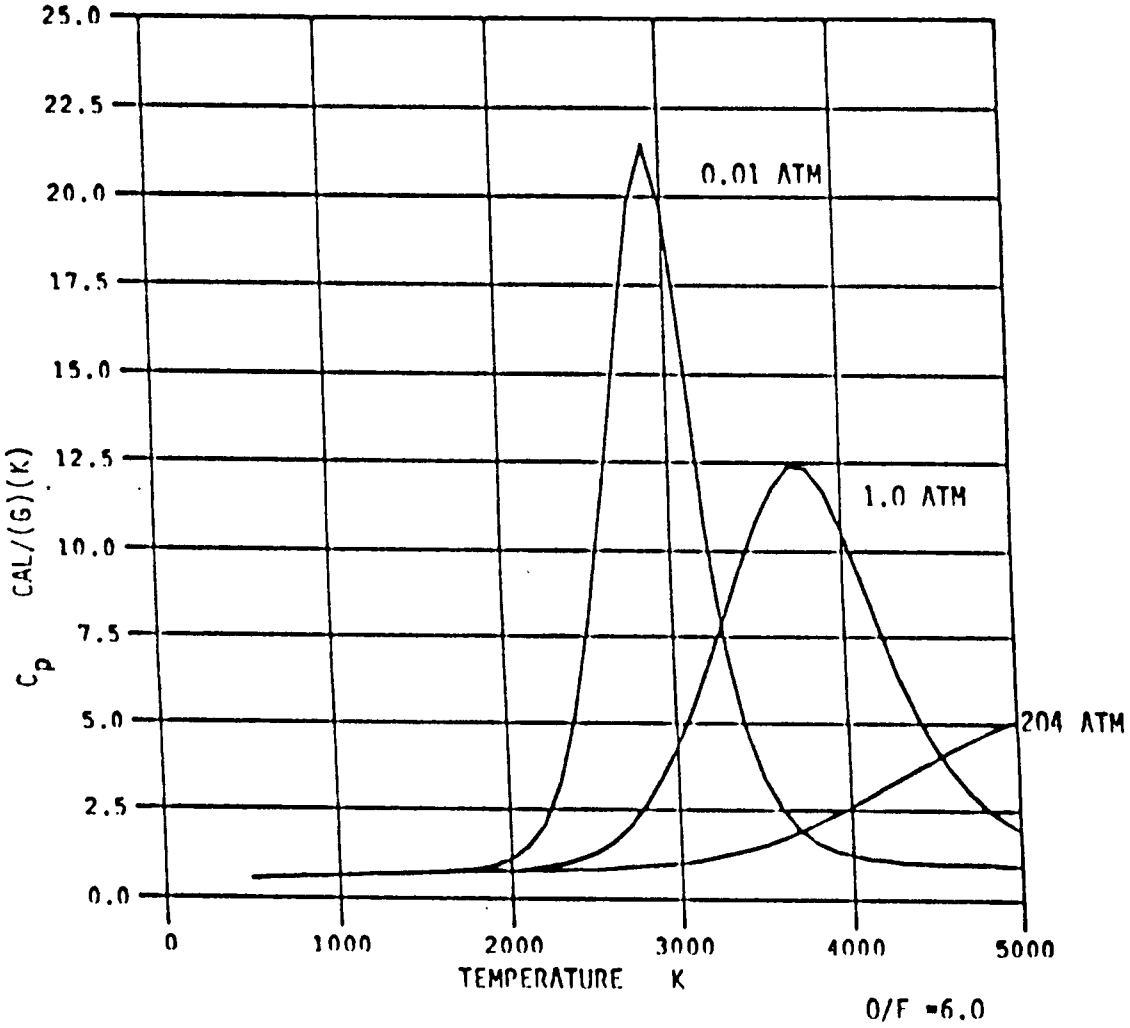


Figure 2. Constant Pressure Specific Heat, C_p

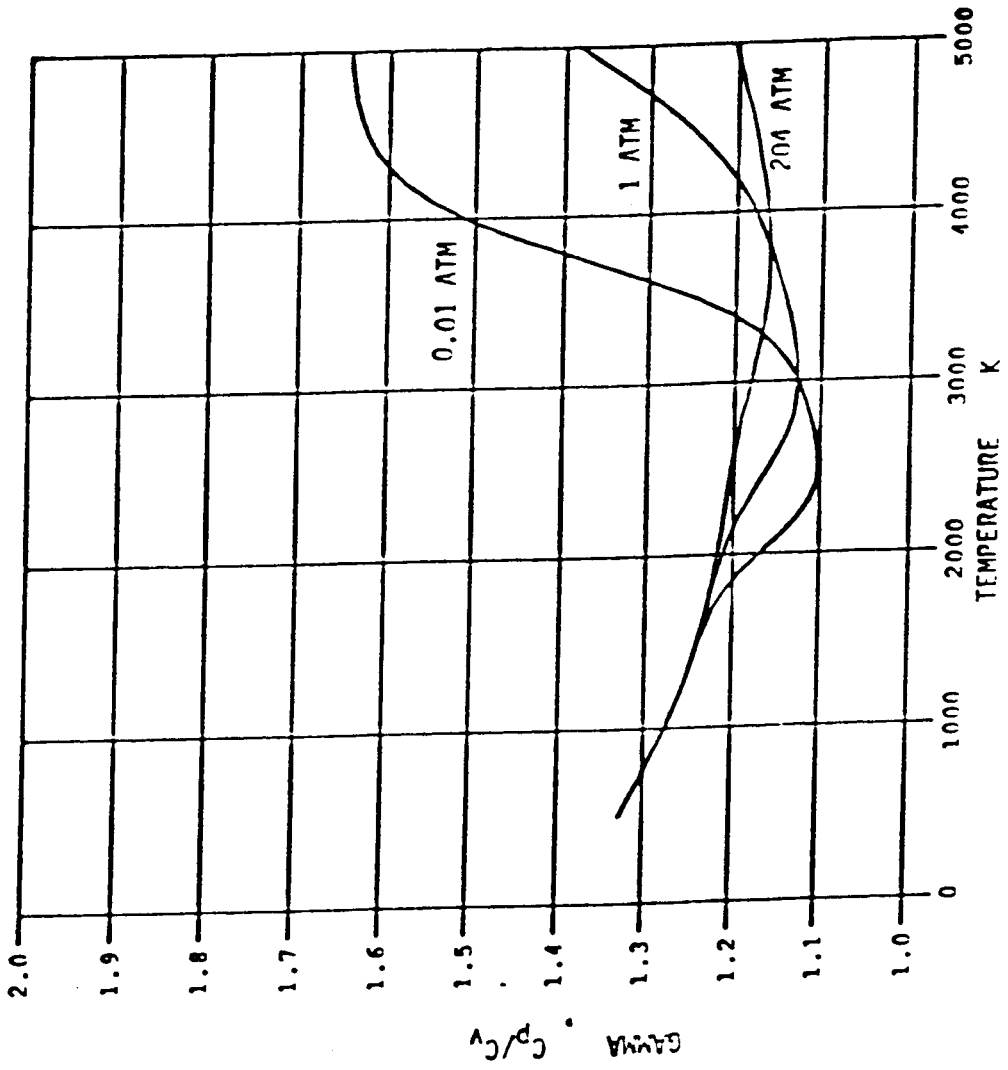


Figure 3. Equilibrium Gamma, O/F = 6.0

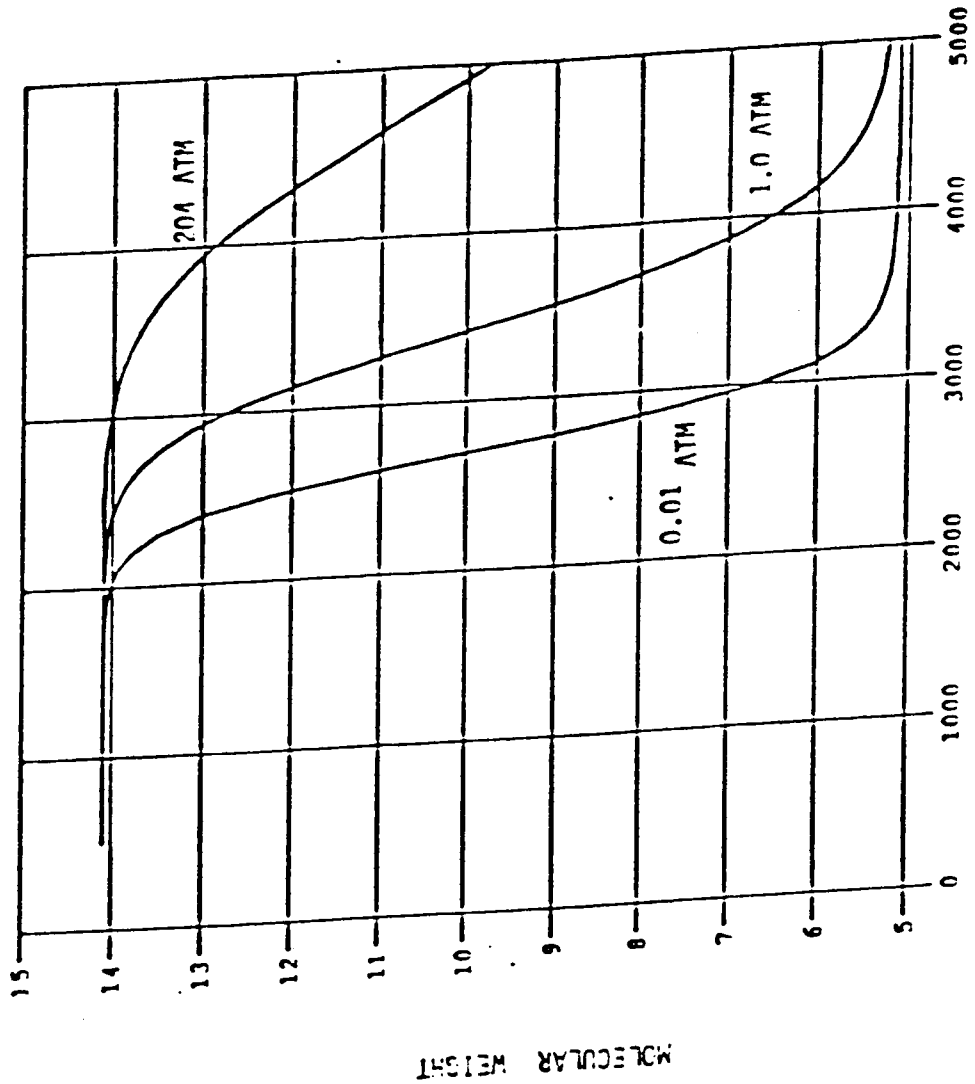


Figure 4. Mixture Molecular Weight, O/F = 6.0

Transport Property Calculations

The transport property section calculates the equilibrium mixture viscosity and thermal conductivity using equations based on kinetic theory. These equations are listed in Appendix E along with the references from which they came.

To proceed with the calculations, the collision integrals for all of the possible binary interactions are required. Data for these collision integrals were taken from [18]. In order to interpolate the collision integrals for viscosity, the data were curve fit by the least squares method into 4th order functions of temperature. Values obtained from the curve fits were within 5% of the actual data. Data for the ratio A^*_{ij} (ratio of collision integrals of viscosity and diffusion) are interpolated linearly.

Since the collision integrals for HO_2 were not readily available and the composition of the flow was determined to have very little HO_2 ($X_{HO_2} < 0.0001$), HO_2 was neglected in the calculations of the transport properties.

Plots of the transport properties are shown in Figures 5 and 6. Comparisons to [18] will show that the results are valid.

Adiabatic Flame Temperature

One of the starting conditions needed by the PARC code is chamber or stagnation temperature. For starting the equilibrium PARC code a routine was added which computes the adiabatic flame temperature of hydrogen-oxygen combustion for the specified chamber pressure and O/F. This temperature is then used as the chamber temperature.

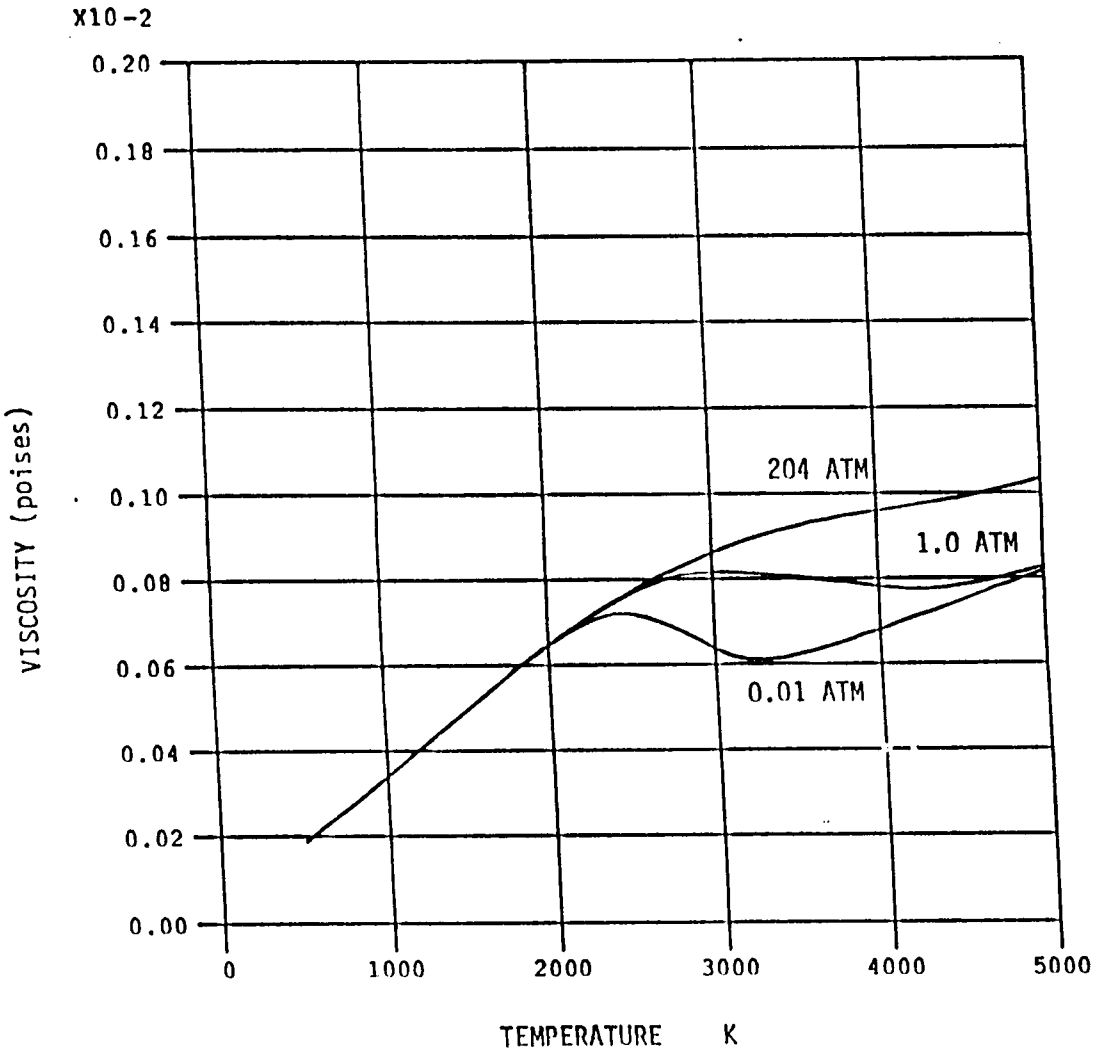


Figure 5. Mixture Viscosity, O/F = 6.0

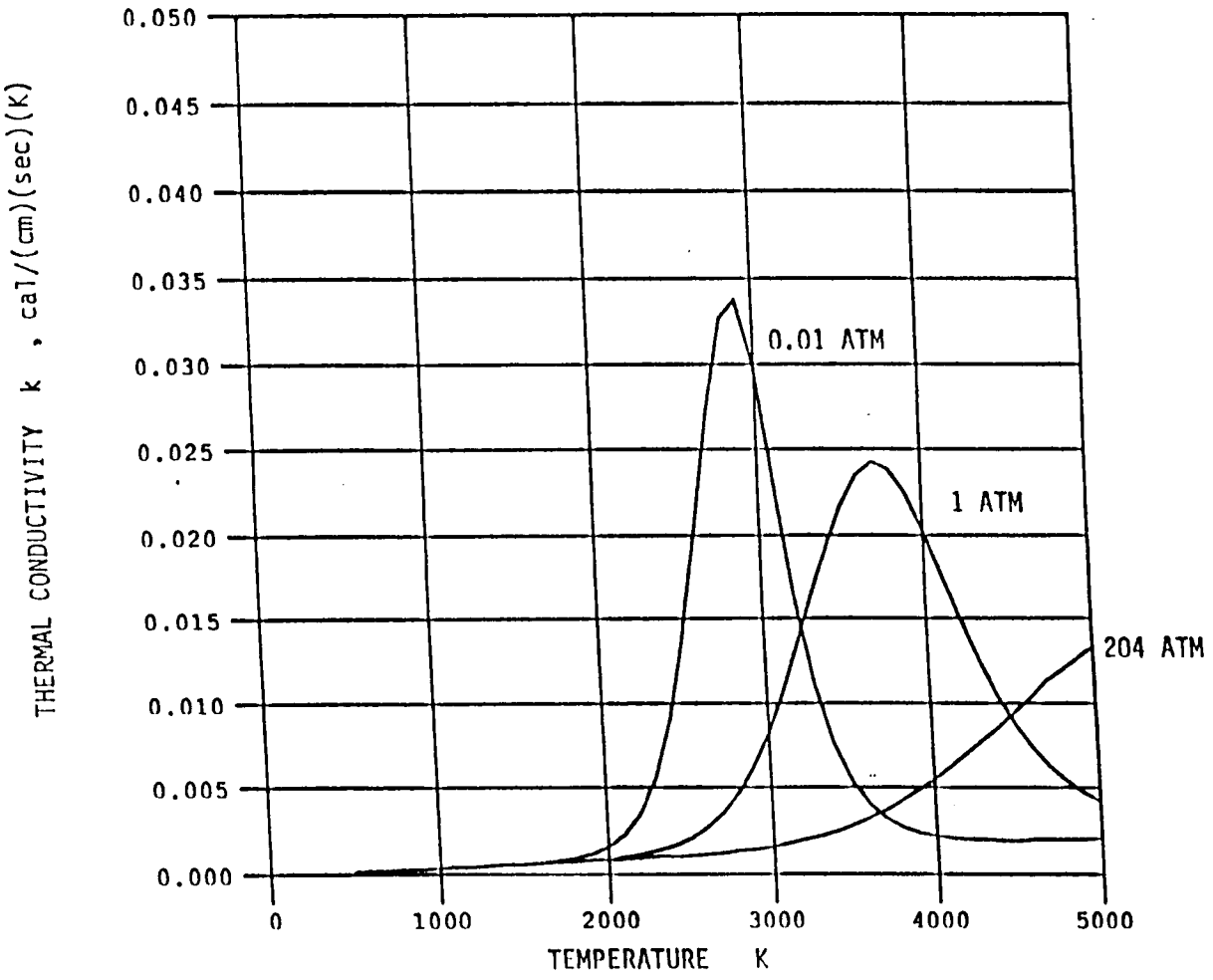


Figure 6. Thermal Conductivity, O/F = 6.0

The equation for finding the adiabatic flame temperature is derived in [14]. It is the First Law of Thermodynamics applied to a closed system of chemical reactions:

$$H_R = H_P$$

H_R = Initial enthalpy of reactants

H_P = Enthalpy of products at adiabatic flame temperature

For the chemical reaction

$$\eta_{R1} H_2 + \eta_{R2} O_2 \rightarrow \eta_1 H + \eta_2 O + \eta_3 H_2 + \eta_4 O_2 + \eta_5 OH + \eta_6 H_2 O + \eta_7 HO_2$$

The flame temperature equation from above becomes:

$$\sum_{reactants} \eta_i \left[\bar{h}^{o}_{i_f} + \Delta h_i \right]_{initial} = \sum_{products} \eta_i \left[\bar{h}^{o}_{i_f} + \Delta h_i \right]_{end}$$

η_i = number of moles of species i.

To solve for the final temperature, the initial temperature or enthalpy of H_2, O_2, and O/F must be known. This gives a value to the left hand side of the equation. The method of bisection (Appendix F) is used to solve the equation for temperature. At each new iteration for temperature a new composition and enthalpy are calculated for the right hand side of the equation using the previously discussed equilibrium calculations. The flame temperature routine iterates until the absolute error on the adiabatic flame temperature associated with the method of bisection is less than 1°K.

When the adiabatic flame routine is called, the program assumes that a new set of calculations has begun and it assigns the chamber properties to every node of the grid so that computations can begin. The chamber properties are also used as the reference properties for the nondimensionalization of the code. Appendix G gives the actual equations for the nondimensionalization.

The Variable Beta (β)

One of the most important variables calculated in the equilibrium section is B. It is defined as the ratio of enthalpy to internal energy, $\beta = h/e$ [4]. It takes the place of the ratio of specific heats, γ, in the original PARC code since γ is no longer considered to be constant. Beta is related to the pressure by the equation

$$P = (\beta - 1)\rho e$$

and appears frequently in the flux Jacobian matrices of the code.

The conversion from γ to β posed some initial problems in the calculations because of negative values of β. These problems were ultimately solved by changing the reference state from which h and e are calculated. Sixty thousand (60,000) cal/gm-mole was added to the heat of formation of each species in the equilibrium mixture, hence,

$$\beta = \frac{h}{c} = \frac{h_{PR} + 60{,}000}{e_{PR} + 60{,}000}.$$

The subscript PR refers to the previous reference state where at 1 atm and 77°F the heat of formation of H_2 and O_2 was taken to be zero. It

should be noted here that the definition of β has not actually changed. The numerical change in the value of β encountered from changing the reference state is offset by the change in numerical values of h and e in the flow solver.

The value 60,000 cal/gm-mole was chosen because it made the heat of formation of water positive and kept the β values positive over the necessary temperature and pressure ranges. This is shown by a plot of β in Figure 7.

Performance Calculations

A performance routine is also added to the code to calculate the following nozzle performance parameters: mass flow, thrust and specific impulse. The performance routine integrates the flow properties along a designated plane in the nozzle (usually the exit plane) using the composite trapezoidal rule. Ambient pressure (P_∞) was taken to be 0.03 psia. It should be noted that results using this method will be dependent on how well the code conserves mass flow through the nozzle.

The following is a list of equations used:

1) Mass Flow, $\dot{m}$

$$\dot{m} = \int \rho V \, dA$$

$\dot{m}$ = mass flow

ρ = density

V = velocity

dA = cross-sectional area

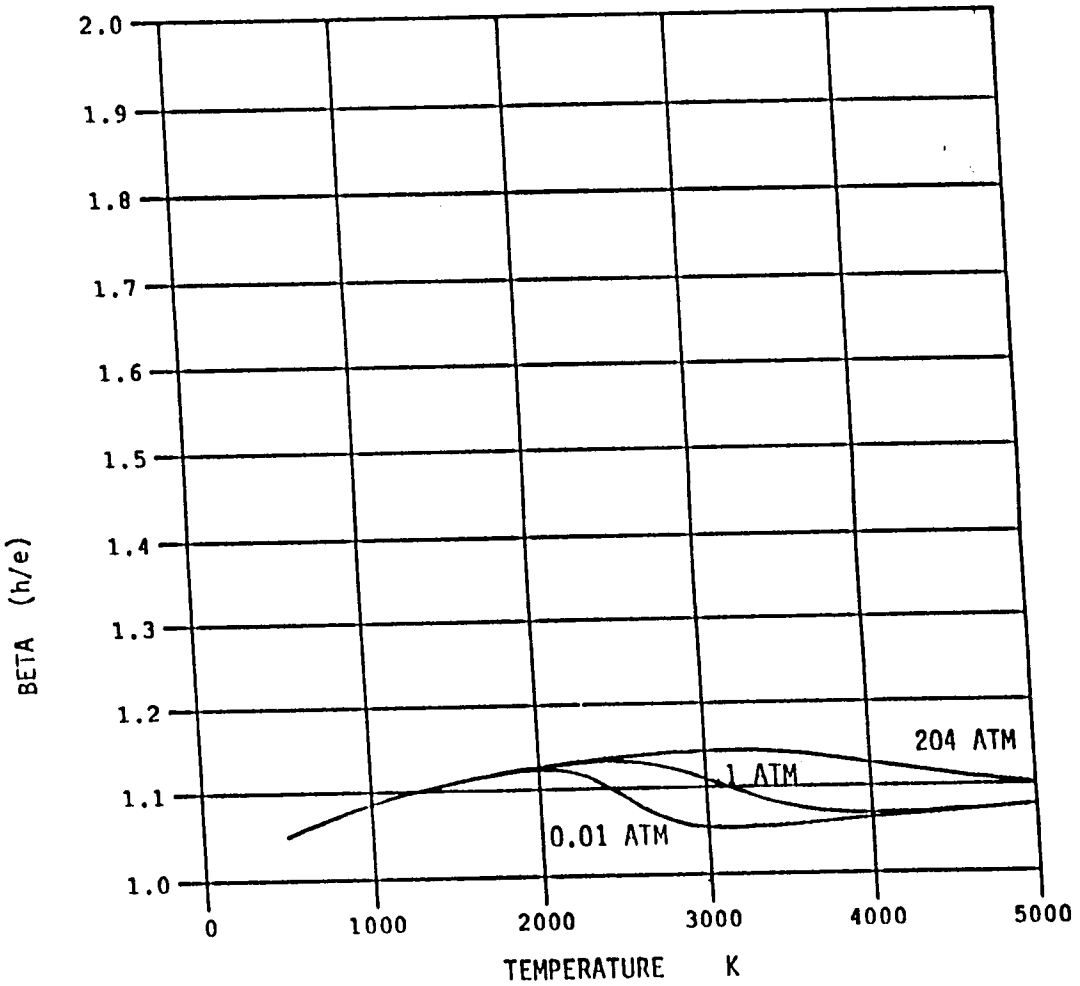


Figure 7. Beta (Ratio of Enthalpy to Internal Energy) versus Temperature

2) Thrust, F

$$F = \int \rho V^2 dA + \int \left(P_e - P_\infty\right) dA$$

P_e = nozzle exit pressure

3) Specific Impulse, I_{sp}

$$I_{SP} = \frac{F}{\dot{m} g_e}$$

g_e = acceleration of gravity at earth's surface.

Added Convergence Parameters

Two factors are added to the equilibrium PARC code to help the convergence. The first (NXPRT) controls the number of times that the equilibrium routine is called by the code. The second (w) is a weighting factor for the relaxation of the temperature change encountered by the equilibrium calculations.

NXPRT. Early on it was found that running the equilibrium routine on every iteration through the nozzle was very time consuming and probably unnecessary. It was decided to limit the number of times the equilibrium routine was called. The input variable NXPRT is used for this purpose. This variable also controls the number of times the convergence statistics are printed [2].

The Weighting Factor (w). The modification of the PARC code for equilibrium air [4] found that a relaxation of the temperature change experienced by the equilibrium routine was needed to provide a converged solution. A similar relaxation method is employed here. The relaxation used the following algorithm:

$$T_E^{N+NXRT+1} = w\,T_E^N + (1-w)T_P^{N+NXPRT}$$

where w is the weighting factor, T^N is the previous temperature, and T^{N+1} is the current temperature. The subscripts E and P denote from which section of the PARC code the temperature applies. The subscript E denotes the equilibrium section and P denotes the fluid-dynamics solver (original PARC). It is important to make sure that the two temperatures are matched at the time of a final converged solution.

CHAPTER IV

COMPUTATIONS ON THE SSME NOZZLE

Assumptions

The equilibrium computations were performed for the SSME nozzle under the following assumptions: Laminar flow, adiabatic wall, 3000 psia chamber pressure, and an O/F = 6.0. Liquid H_2 with an enthalpy of -1837.66 cal/mole and liquid O2 with an enthalpy of -1884.4 cal/mole were used as inputs in the adiabatic flame temperature routine to start the calculations. The adiabatic flame temperature was found to be 6553°R.

Grid

The grid used for the equilibrium PARC code calculations was created by Orr [3] using the INGRID code developed at the Arnold Engineering Development Center (AEDC) [19]. The grid has 210 x 100 node points and is clustered near the wall and in the region of the shock as computed in the constant gamma flow calculations. It is the case 2 laminar grid described in [3].

Convergence Procedure

Throughout the convergence process the temporal time step option was used. This option is controlled with two main variables, DTCAP and PQMAX. DTCAP is the maximum time step variable. PQMAX is the maximum percentage change allowed in density or pressure. PQMAX is used to

stabilize the calculations through the initial rapidly changing part of the convergence process.

In the initial stage of calculations the equilibrium routine was called every 1000 iterations. PQMAX was 25% during this stage. Once the flow field became relatively stable (the convergence statistic L2-residual [2] started to oscillate), PQMAX was lowered to 10% and the equilibrium routine was called every 100 iterations. Again the flow field became relatively stable. For the remaining iterations, DTCAP was lowered enough to control the maximum pressure/ density change.

The code was found to work well with very little temperature relaxation. The weighting factor, w, which seemed to work best through all of the early stages was w = 0.35.

Calling the equilibrium routine every 25 iterations and raising w to a value of 0.65 was the final step used in the calculation of the flow field solution. The procedure was terminated when the value of the L2-residual became less than 10^{-7}. Maximum change in the flow field properties of temperature and pressure for every 100 iterations was less than 0.01%.

Results and Comparisons

The results of the equilibrium PARC code calculations for the SSME nozzle were very much as expected. The most interesting find was the location of the shock inside the nozzle. It was found to reflect off the centerline just before the exit plane of the nozzle. The previous constant gamma calculations with the same grid [3] showed a much different location of the shock. Mach number contours of both solutions

are shown in Figure 8. In explaining the different positions of the shock in the two solutions, it is convenient to think of a series of expansion and compression waves inside the nozzle as in Figure 9. Energy release associated with the equilibrium reactions lead to an increase in the expansion wave angles ("stronger" expansion waves). The increased angles result in the movement of the shock closer to the throat.

Previous work with the SSME nozzle by Chan and Freeman [20] assumed an axial variation of gamma, molecular weight and wall temperature as determined from a one-dimensional chemical equilibrium solution. Figure 10 is a Mach number contour plot of this solution. No discernible shock structure can be recognized. One possible reason for the differences may be that a much coarser grid was used in the calculations of Chan and Freeman.

The chemistry of the nozzle was found to change very little through the last 75% of the expansion process. This is shown by a molecular weight contour plot in Figure 11. The shock, although it significantly changed the temperature, Mach number and gamma at the centerline exit (Figures 12, 13, and 14), is not strong enough to cause a change of the mixture's fully reacted state. This is seen from the molecular weight plot along the centerline (Figure 15).

The performance of the nozzle based on the equilibrium calculations was, as is generally expected, higher than that of the constant gamma solution. This can be shown by a comparison of exit velocities of the two solutions (Figure 16). In the equilibrium solution, energy

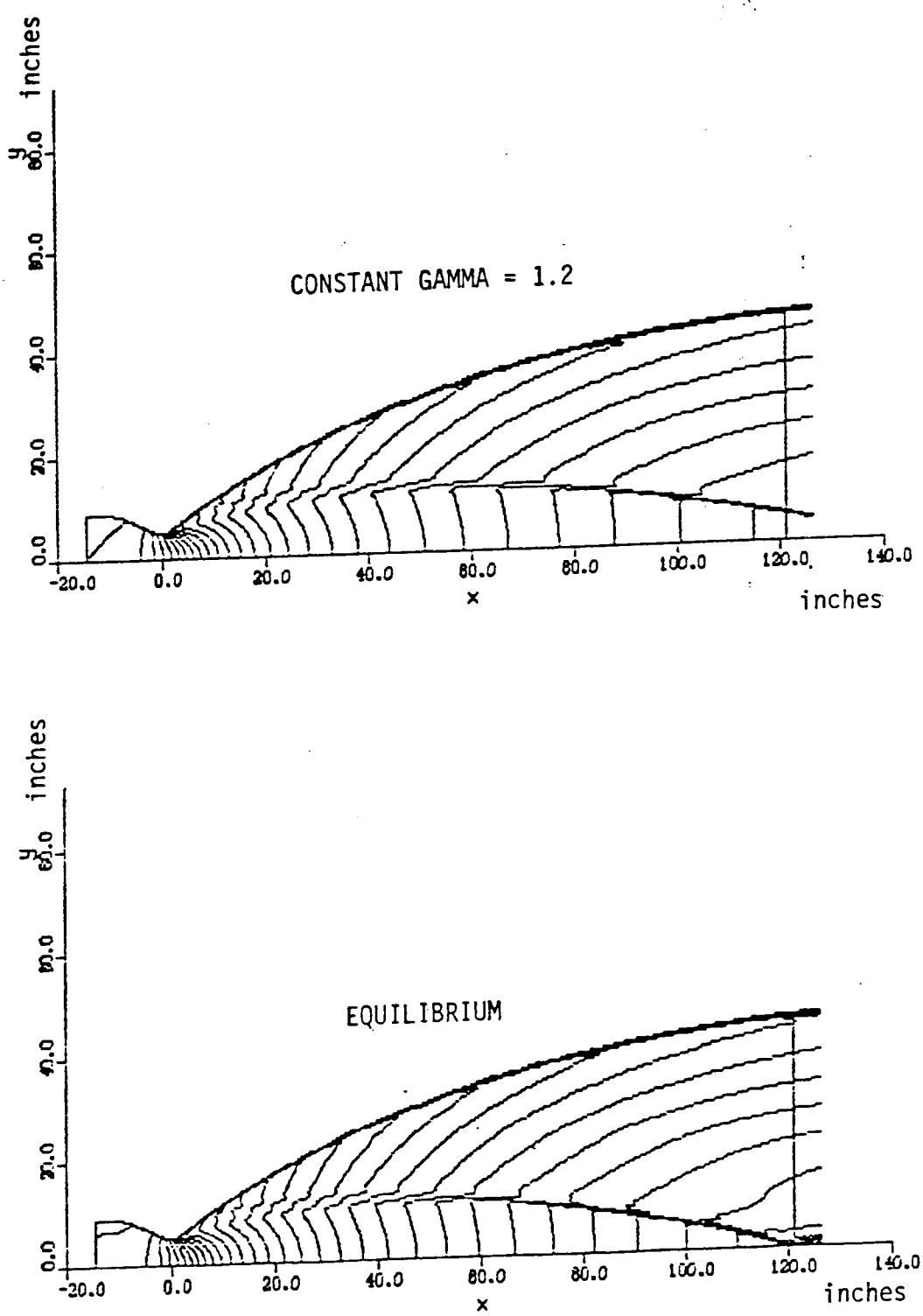


Figure 8. Mach Number Contour Comparison

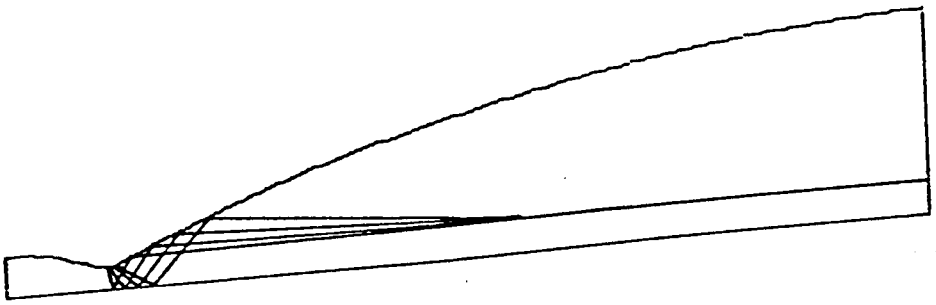


Figure 9. Series of Expansion and Compression Waves Inside a Nozzle with an Internal Shock

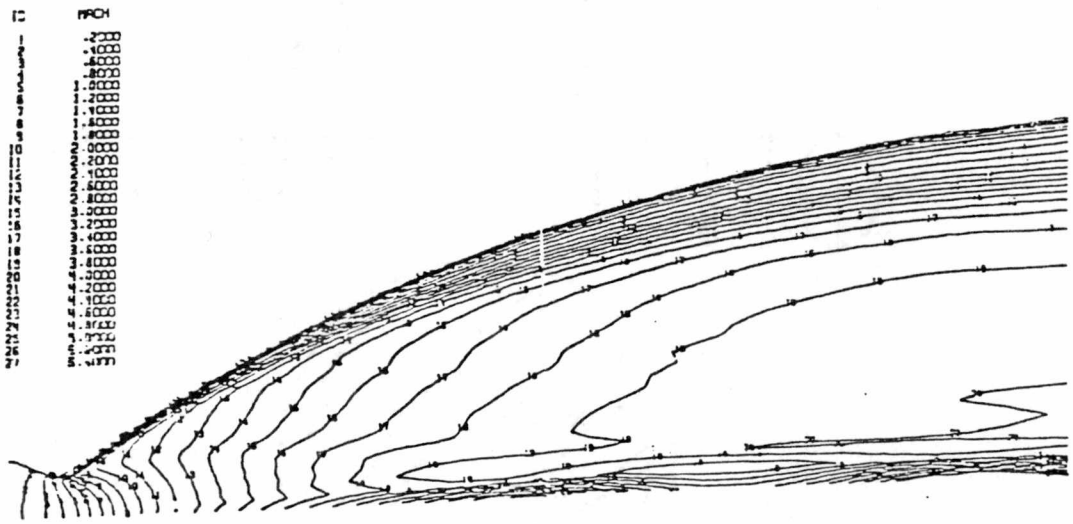


Figure 10. Mach Contour from [17] Axial Gamma Variation, Coarse Grid

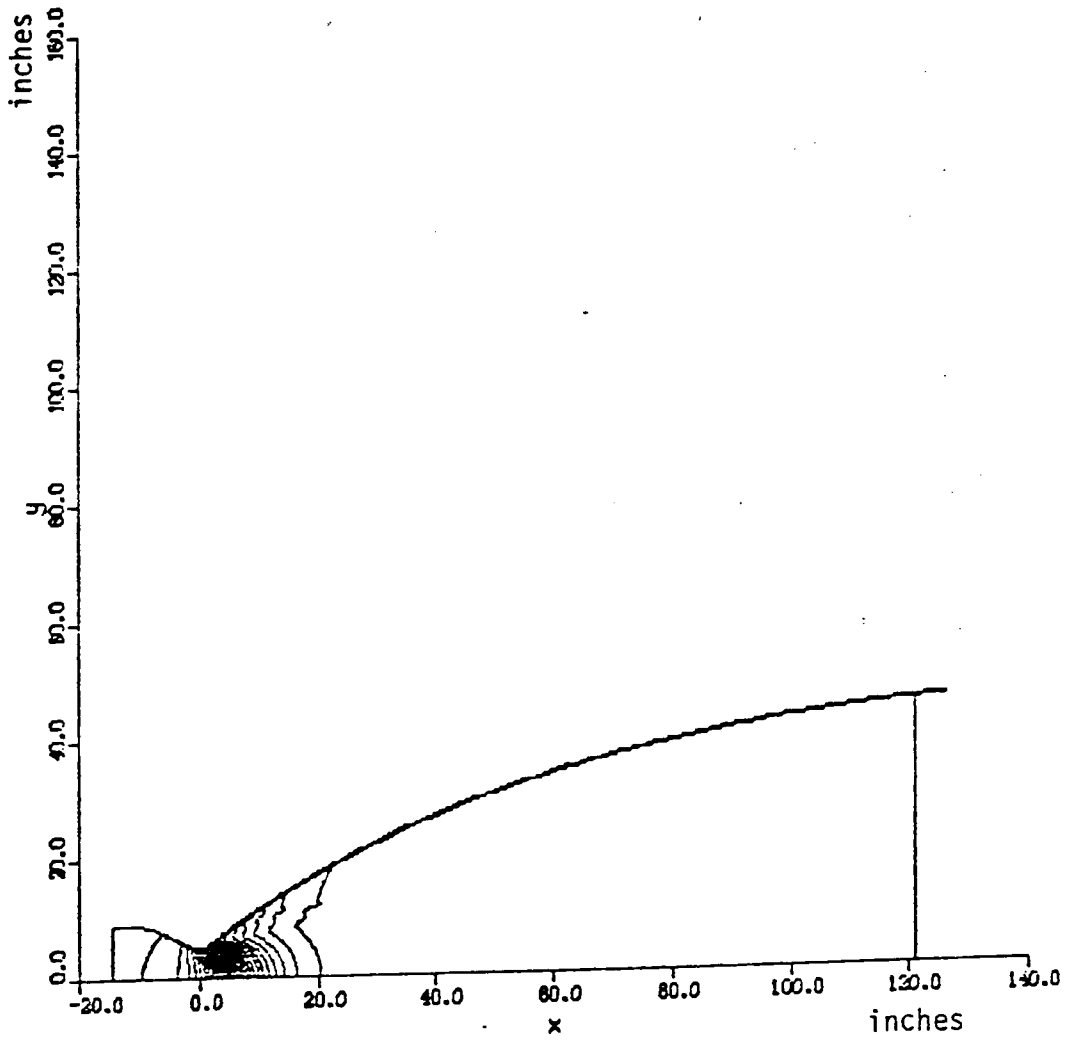


Figure 11. SSME Molecular Weight Contour

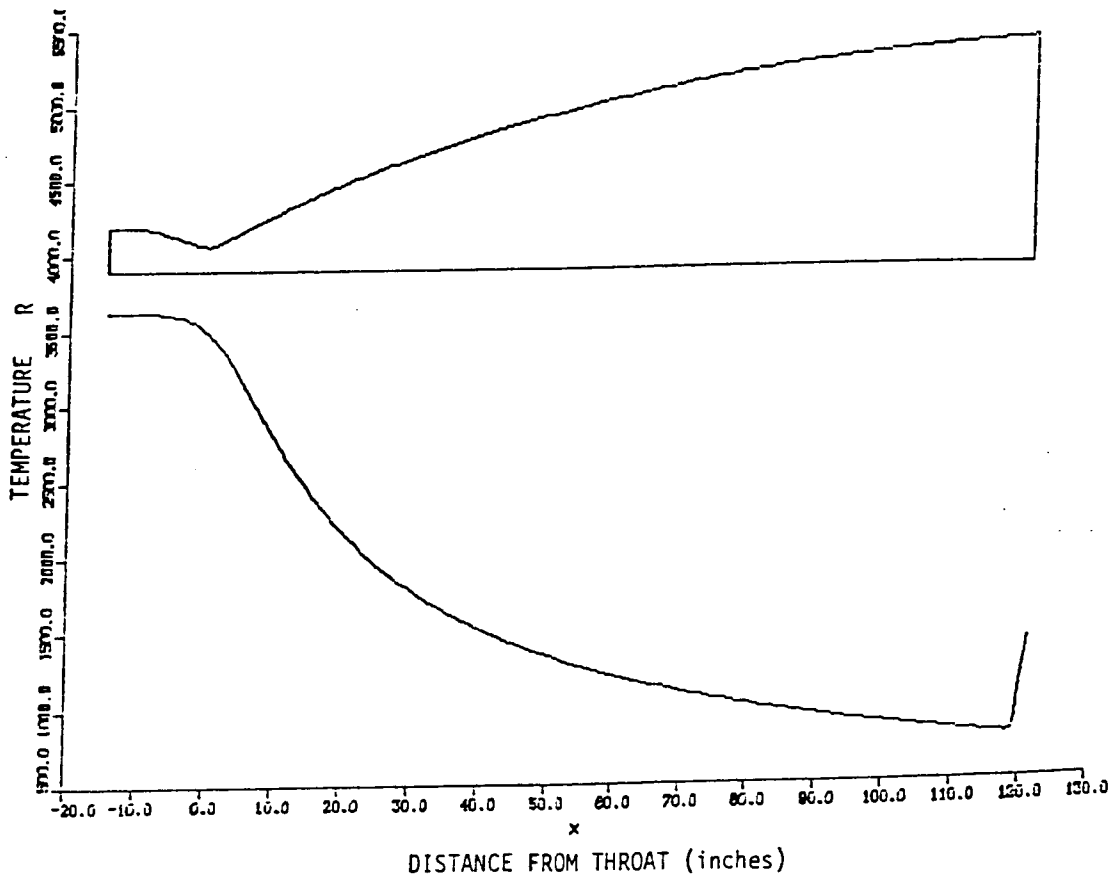


Figure 12. SSME Temperature Along Centerline, Equilibrium

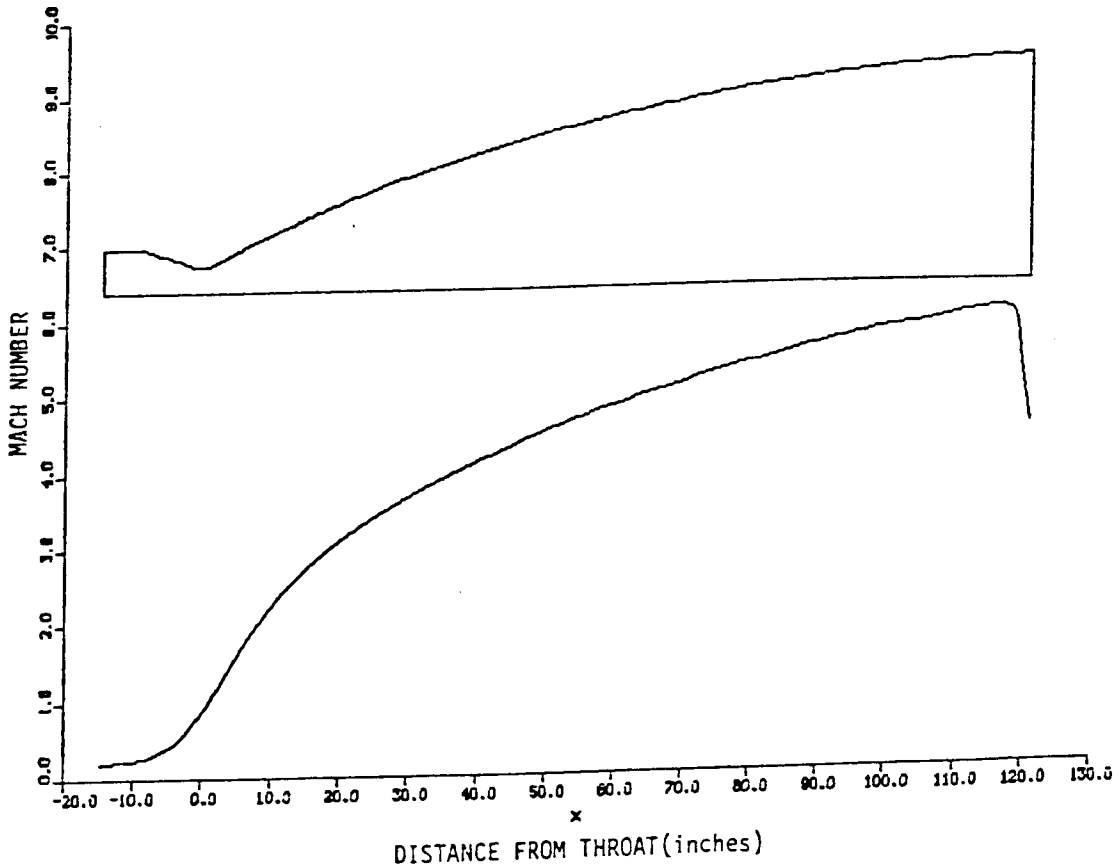


Figure 13. SSME Mach Number Along Centerline, Equilibrium

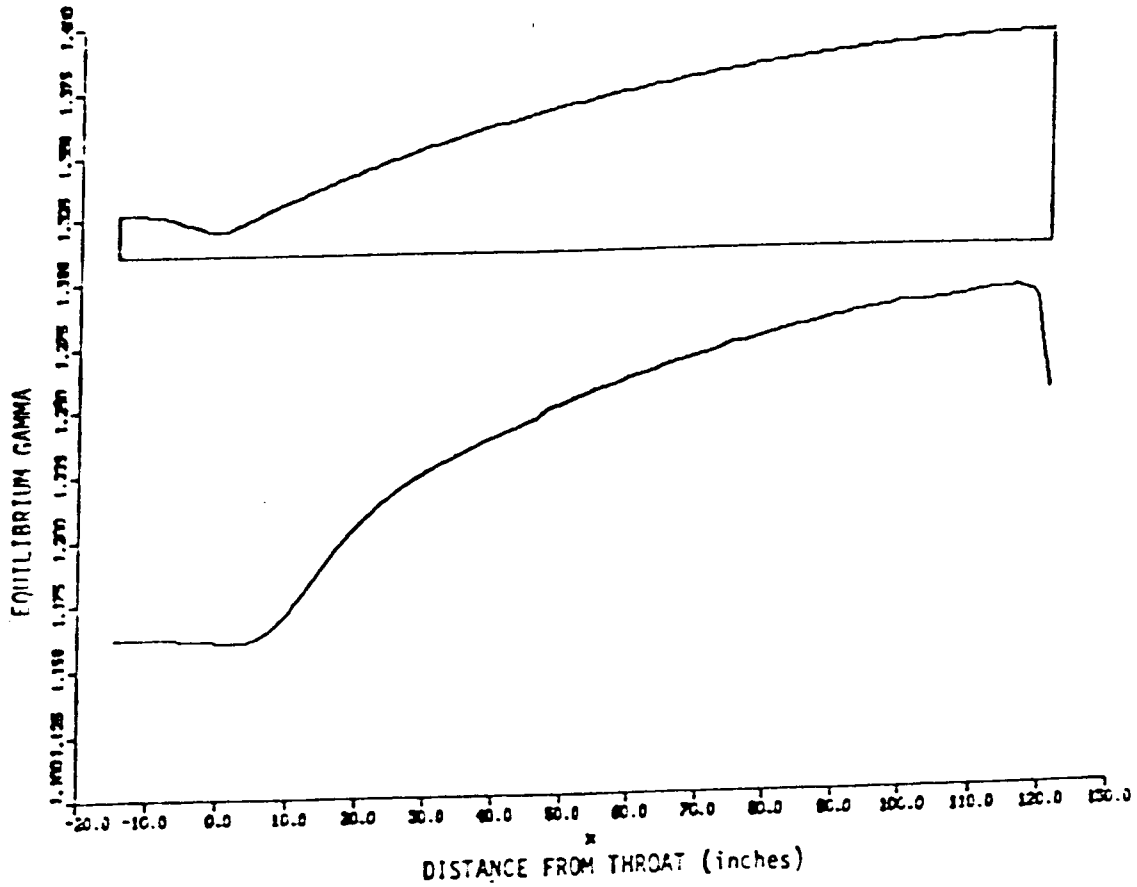


Figure 14. SSME Equilibrium Gamma Along Centerline

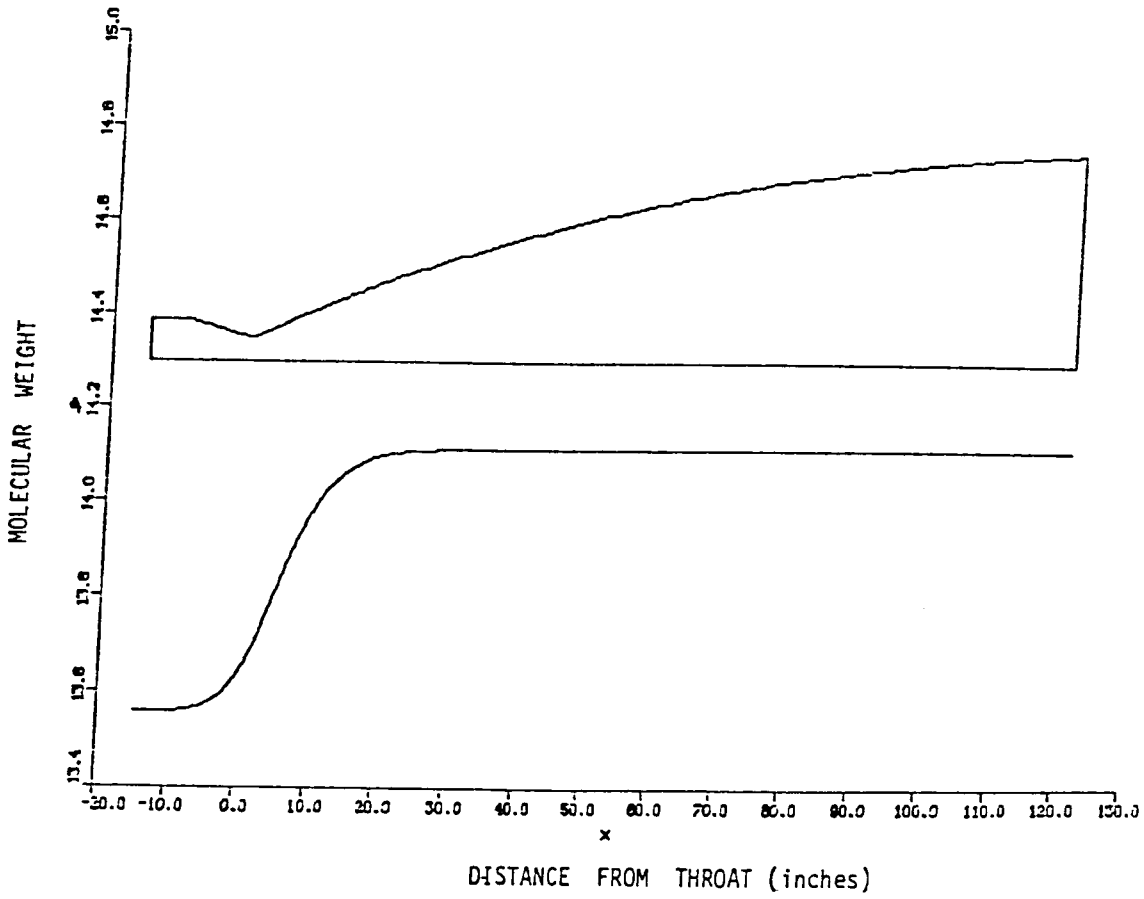


Figure 15. SSME Molecular Weight Along Centerline, Equilibrium

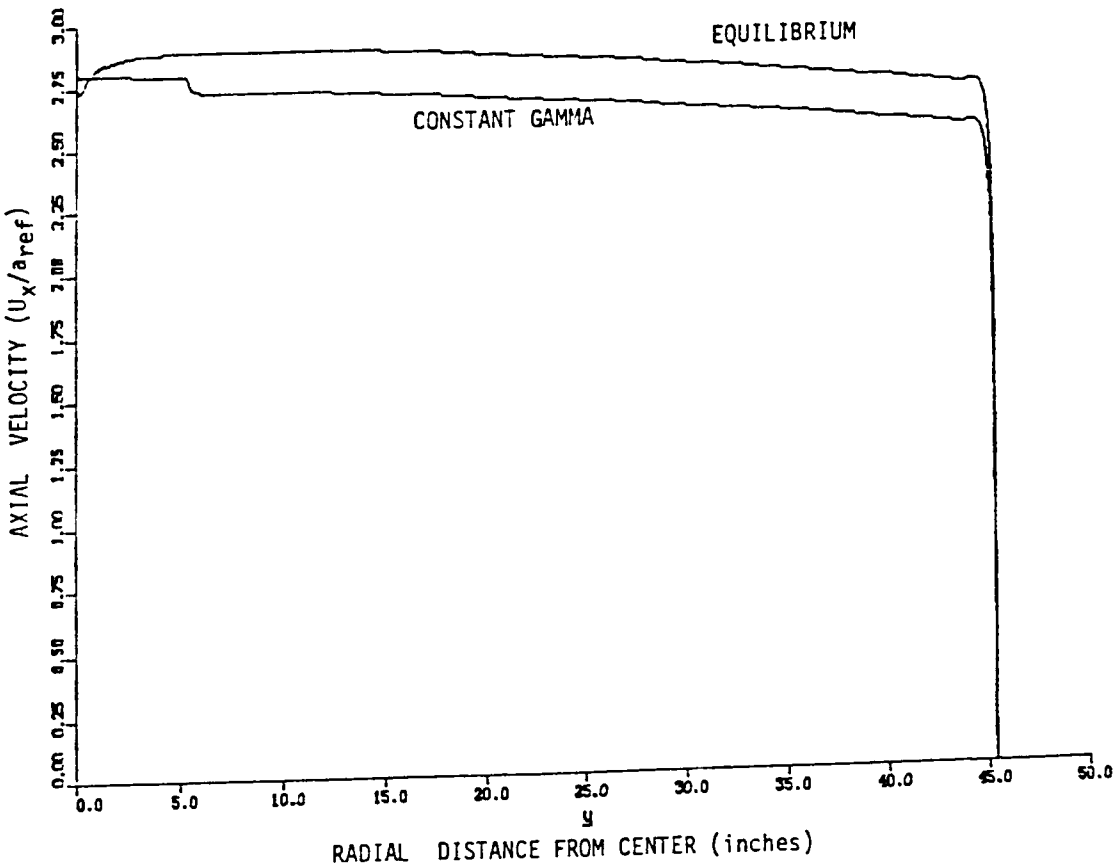


Figure 16. Comparison of Exit Velocities

is released to the flow by the chemical reactions so a higher exit velocity can be achieved since the overall flow is adiabatic. Assuming a constant gamma flow implies the chemistry is "frozen" at some thermodynamic state so no energy is released during expansion. This is shown clearly in Figures 17 and 18, which compare the temperature and velocity of the two solutions along the centerline of the nozzle. Figures 17 and 18 are important figures because normally a finite rate chemistry (nonequilibrium) solution will be bound by these two solutions. Of course, the finite rate chemistry solution will most accurately model the real flow.

Performance parameters of several different solutions and the measured test data are shown in Table 2. As expected, the measured performance is bound by the equilibrium and constant gamma solutions. The TDK code performance parameters were obtained by running the TDK code with the same inputs used for equilibrium PARC. The results of TDK and equilibrium PARC are in reasonable agreement, but more investigation is needed to determine the specific nature of the differences. The results of Chan and Freeman seem to be poor.

As noted in the Performance Routine section, the accuracy of performance parameters calculated by equilibrium PARC is dependent on how well mass flow is conserved by the code. The difference between the calculated inlet and exit mass flows is most likely due to the errors associated with the numerical integration (trapazoidal rule described in Performance Calculation Section) across the grid nodes. Regardless,

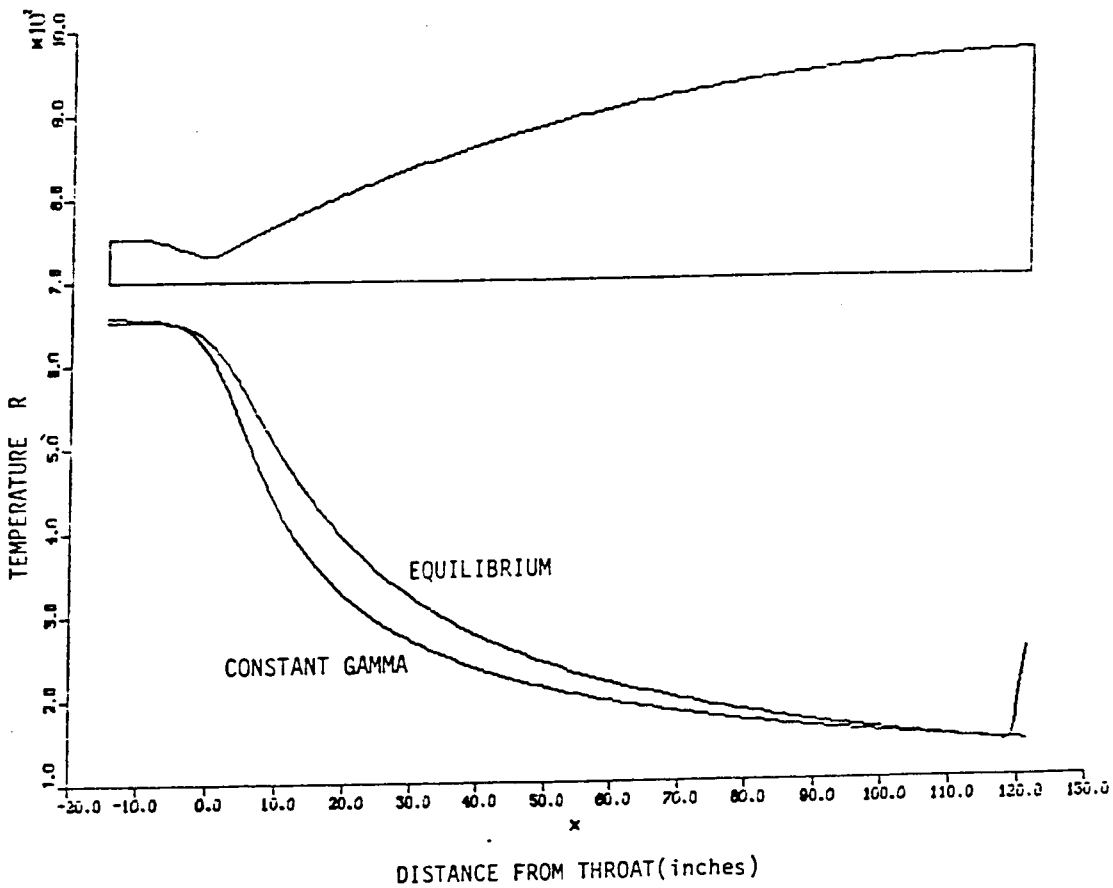


Figure 17. Temperature Comparison Along Centerline

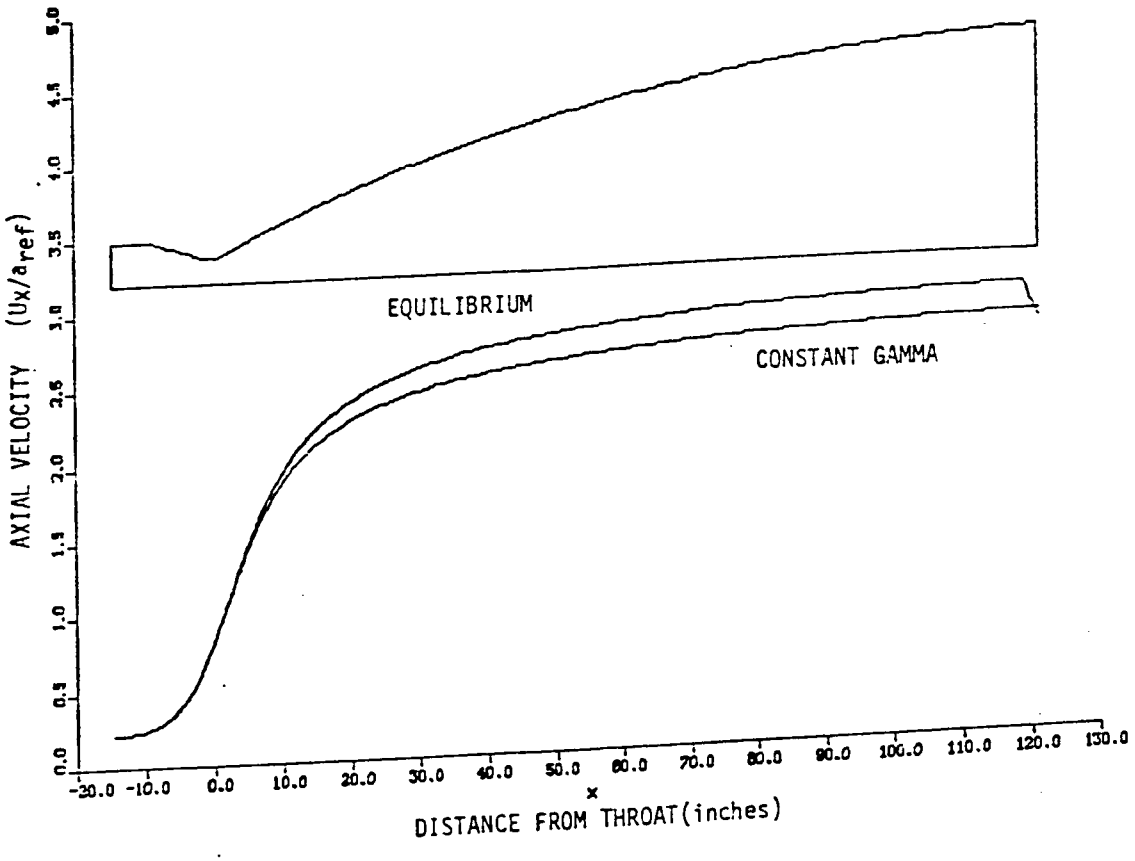


Figure 18. Centerline Axial Velocity Comparison

Table 2. Comparison of Performance Parameters

	$\dot{m}$(lb/s)	Thrust (lbf) (10^6)	I_{sp} (sec)
PARC2D, Laminar Constant γ w/EADM [6]	1071.5	4.754	443.7
PARC2D, Laminar Equilibrium	1031	4.867	471.9
Test Data [21]	1039.5	4.698	452
TDK, laminar	1036.9	4.821	465
Chan and Freeman [20]	978	5.12	523

a comparison of the inlet and exit mass flows gives an indication as to the accuracy of the performance parameters. Mass flow calculated by the Performance Routine at the nozzle inlet was 1025 lbm/s. The exit mass flow was 1031 lbm/s. The relative error of the two mass flows

$$error = \left(\frac{\dot{m}_{inlet} - \dot{m}_{exit}}{\dot{m}_{exit}} \right)$$

is 0.006, which is within the expected errors associated with the numerical integration.

The equilibrium solution boundary layer was examined at the exit plane. Comparisons were again made with the constant gamma solution. Both solutions employed laminar calculations. The results show that, although the free-stream properties (temperature and velocity) are different, the boundary layer thicknesses are almost equal (Figures 19 and 20).

Since the free-stream properties were different, the results were normalized in Figures 21 and 22 to provide a more appropriate comparison. It is clear that the different velocity profiles are due to the different free-stream velocities being distributed over the same boundary layer thickness. The different temperature profiles are caused by the changing chemistry across the boundary layer in the equilibrium solution and differences in the thermal conductivity. Figures 23 and 24 show how molecular weight and gamma change across the boundary layer. Dissociation absorbs some of the energy and thus flattens the temperature profile in the high temperature region near the

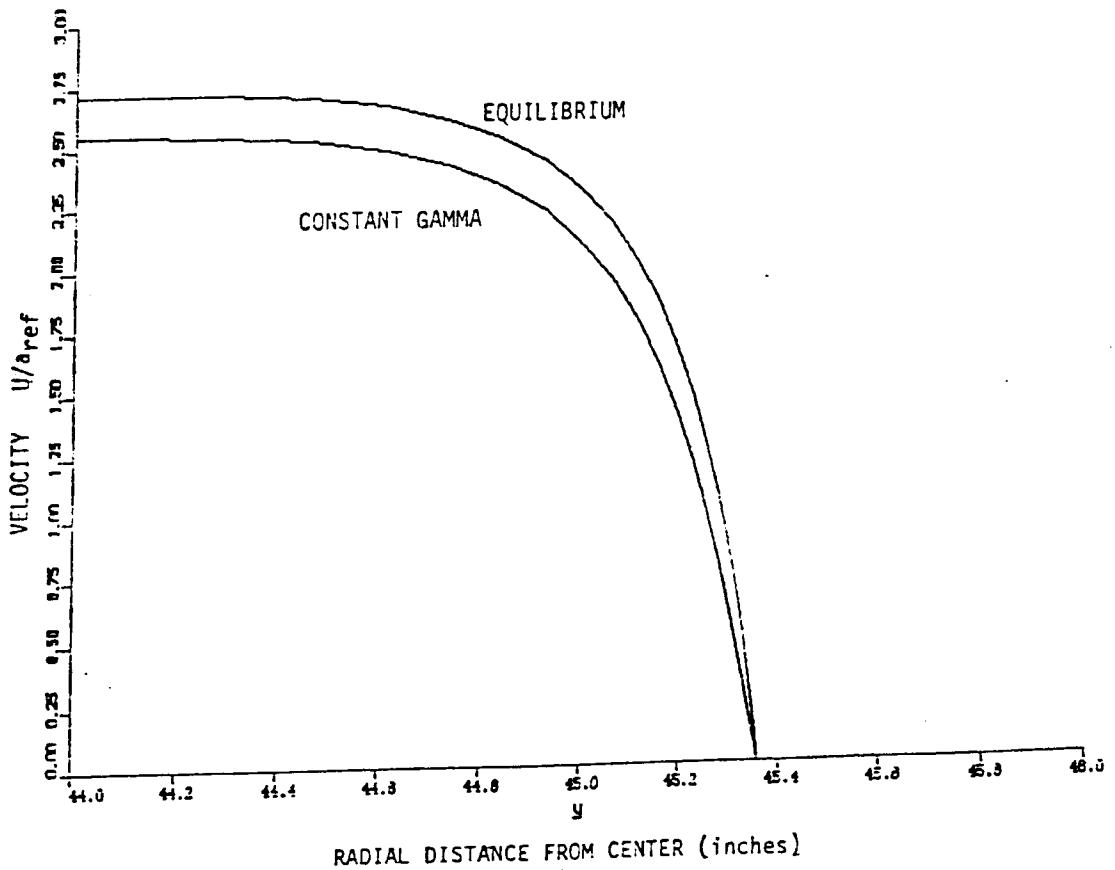


Figure 19. Velocity Profiles in Boundary Layer, Exit Plane

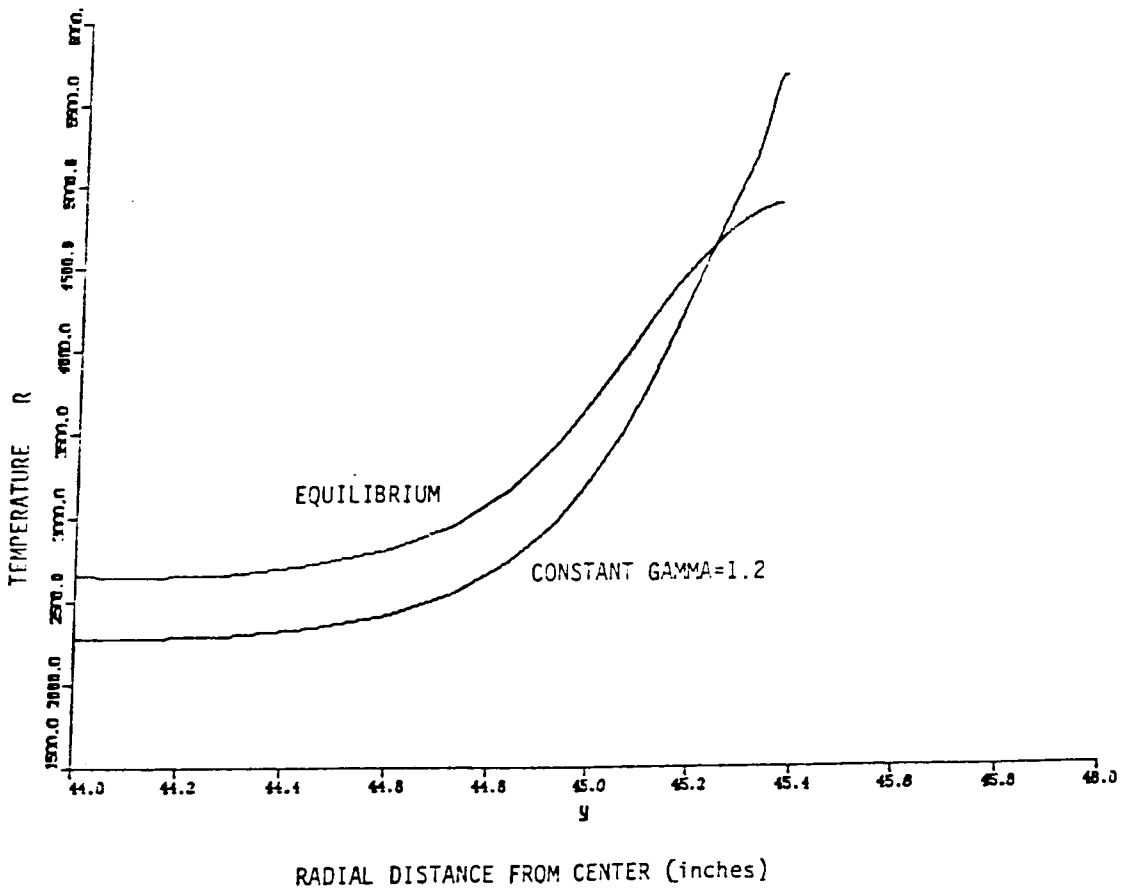


Figure 20. Temperature Profile in Boundary Layer, Exit Plane

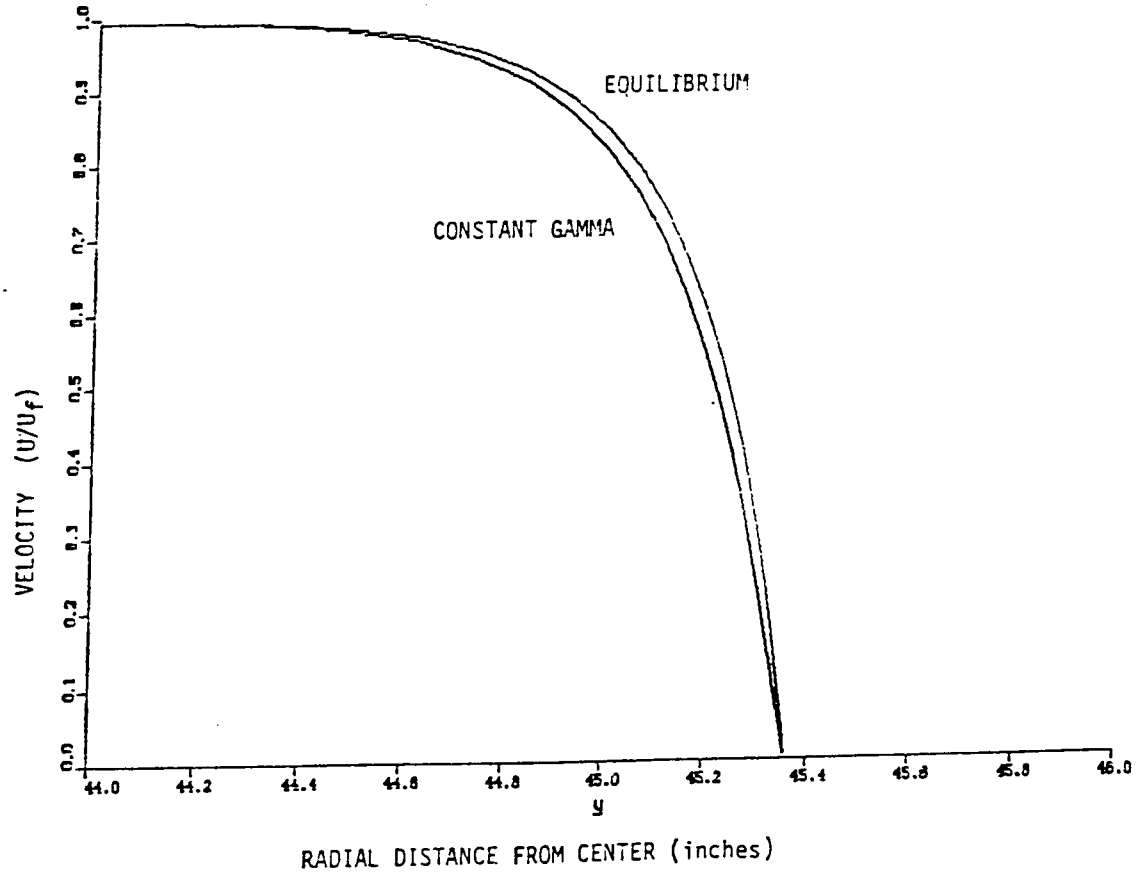


Figure 21. Normalized Velocity Profile in Boundary Layer, Exit Plane

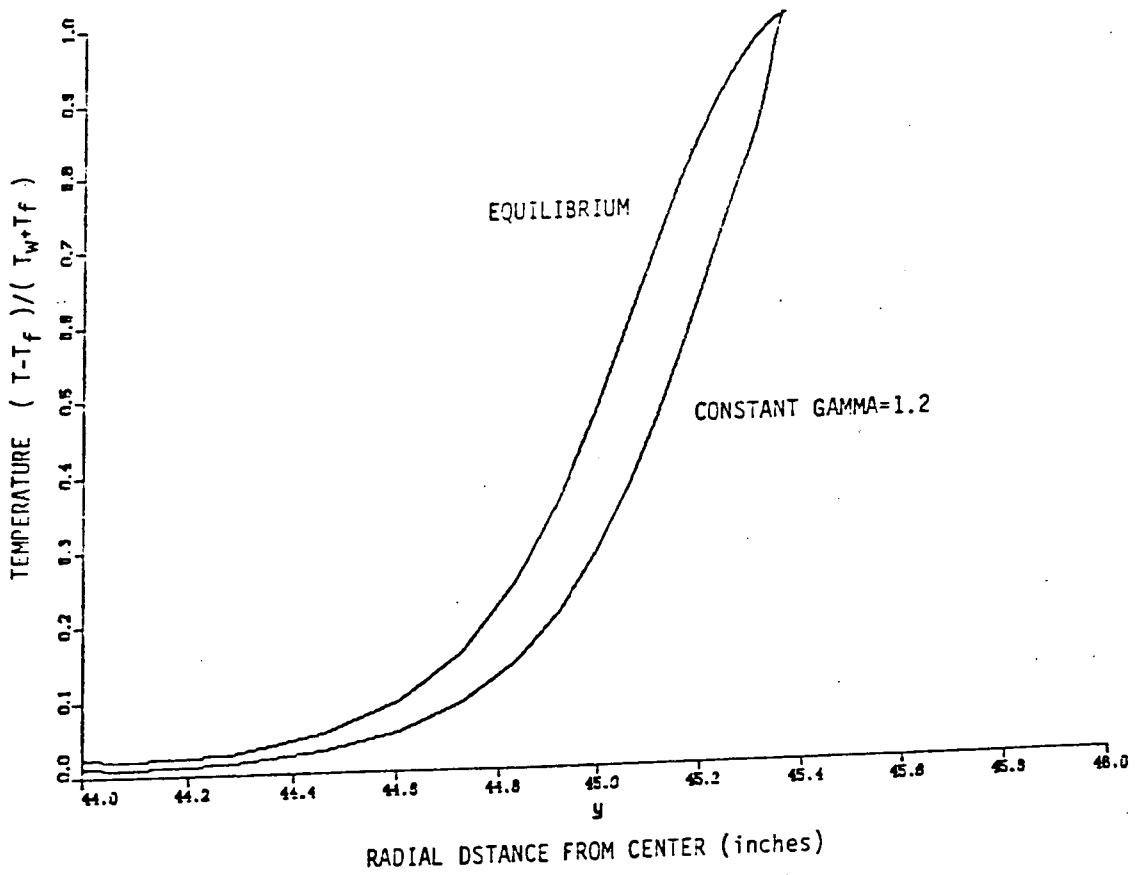


Figure 22. Normalized Temperature Profiles in Boundary Layer, Exit Plane

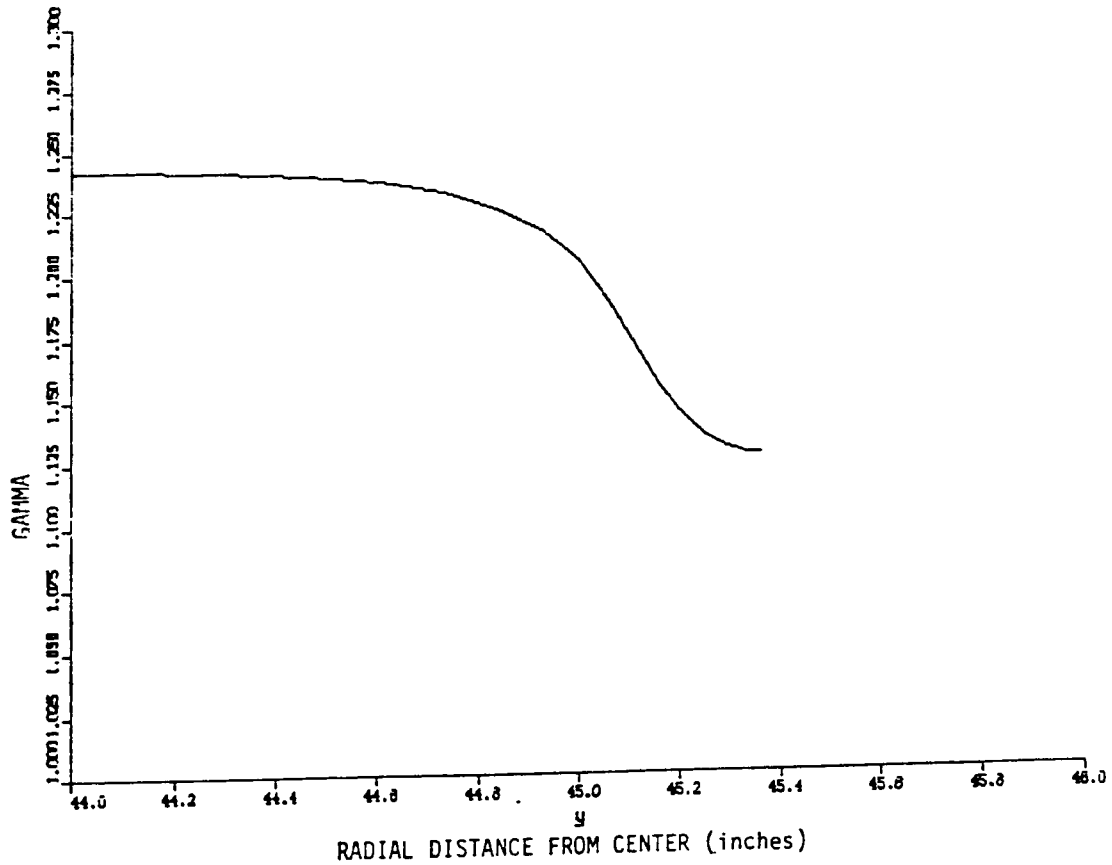


Figure 23. Equilibrium Gamma Across the Boundary Layer, Exit Plane

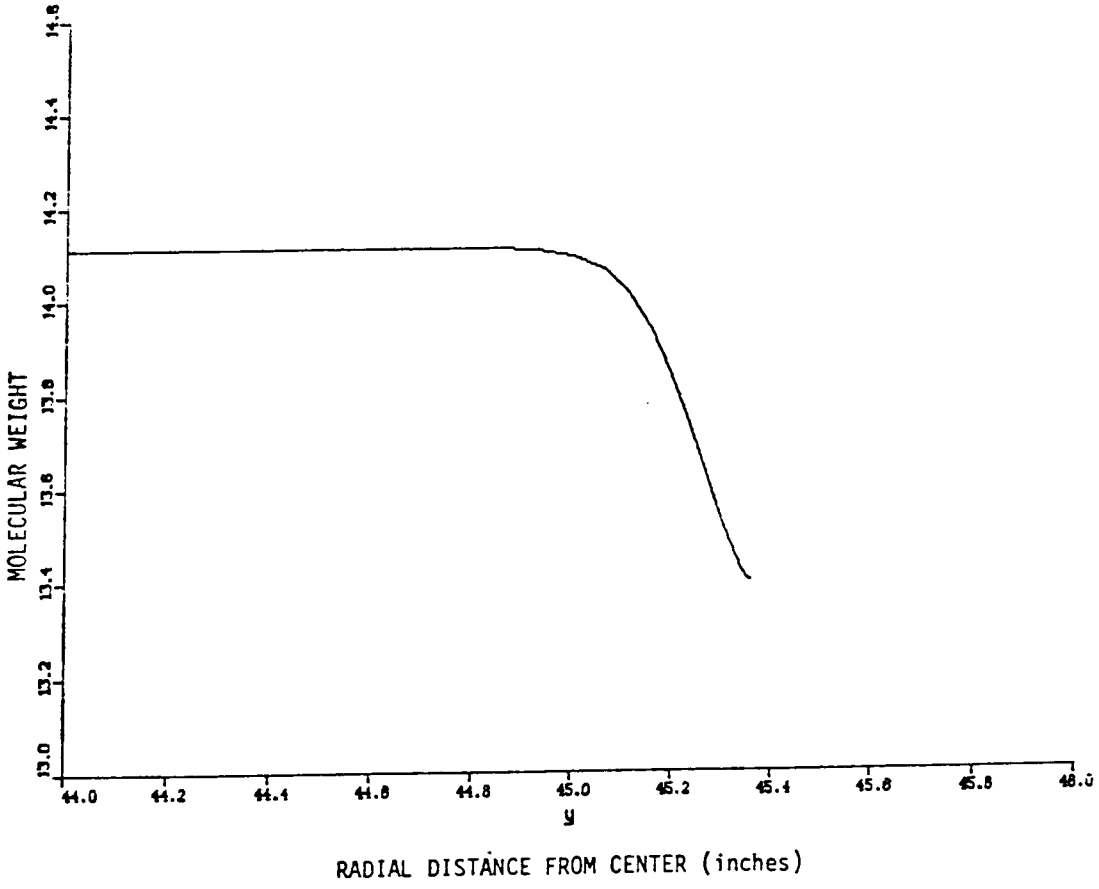


Figure 24. Molecular Weight Across the Boundary Layer, Exit Plane

wall. Dissociation also increases number density which increases reactive thermal conductivity, further flattening profile.

More analysis of the boundary layer was done in [6]. The results suggest that the grid used was too coarse to correctly compute the boundary layer for either PARC code solution; however, the general trends of the boundary layer comparisons which have been made should still be valid.

CHAPTER V

SUMMARY AND CONCLUSIONS

The PARC2D Navier-Stokes code was extended to model hydrogen-oxygen equilibrium reacting flows. The usefulness of the new version of the code was demonstrated on the SSME nozzle. Results, as compared to the previous constant gamma calculations from PARC2D and using the same grid, are summarized as follows:

1) There is change in the shock location. The shock from the equilibrium solution reflects off the centerline just before the exit of the nozzle.
2) Higher performance is calculated from the equilibrium solution due to energy release by the chemistry.
3) The calculated laminar boundary layer thicknesses are almost equal.
4) The calculated laminar boundary layer temperature profiles are different because of the changing chemistry of the equilibrium solution across the boundary layer, i.e., dissociation.

The next steps toward improvement of the results would be to:

1) Introduce the known wall temperature profile instead of assuming an adiabatic wall.
2) Improve the grid (more nodes near the wall to correctly calculate the boundary layer).

3) Run the turbulent boundary layer option of PARC2D with equilibrium to compare to the laminar solution.

4) Analyze the importance of finite rate chemistry and incorporate it into the code provided the computational benefits are justified.

LIST OF REFERENCES

LIST OF REFERENCES

1. Nickerson, G. R., Coats, D. E., and Dang, L. D., "Two-Dimensional Kinetic Reference Computer Program (TDK)," NASA CR-178628, 1985.

2. Cooper, G. K., "The PARC Code: Theory and Usage," AEDC-TR-87-24, Arnold Engineering Development Center, Tullahoma, Tennessee, October 1987.

3. Orr, J. L., "SSME Nozzle Flow Field Calculations Using PARC CFD Code," M. S. Thesis, The University of Tennessee, Knoxville, Tennessee, December 1989.

4. Salandino, A. J. and Praharaj, S. C., "Upgrade to PARC2D to Include Equilibrium Real Gas Effects," Remtech, Inc., Huntsville, Alabama, Report RTR 181-02, January 1990.

5. Cooper, G. K. and Sirbaugh, J. R., "PARC Code: Theory and Usage," AEDC-TR-89-15, Arnold Engineering Development Center, Tullahoma, Tennessee, December 1989.

6. Collins, F. G., Orr, J. L., and Myruski, B. L., "Modification of the PARC Navier-Stokes Code to Predict Engine Nozzle Performance," AIAA Paper 90-2491, Orlando, Florida, July 1990.

7. Beam, R. and Warming, R. F., "An Explicit Finite Difference Algorithm for Hyperbolic Systems in Conservative Law Form," J. Conp. Phys. Vol. 22, 87-110 (1976).

8. Pulliam, T. H. and Steger, J. L., "Implicit Finite - Difference Simulations of Three Dimensional Compressible Flow," AIAA Journal, Vol. 18, 1980, pp. 159-167.

9. Pulliam, T. H., "Euler and Thin Layer Navier-Stokes Codes: ARC2D, ARC3D," Proceedings Computational Fluid Dynamics Users' Workshop, The University of Tennessee Space Institute, Tullahoma, Tennessee, March 1984.

10. Jameson, A., Schmidt, W., and Turkel, E., "Numerical Solutions of the Euler Equations by Finite Volume Methods Using Runge-Kutta Time - Stepping Schemes," AIAA Paper 81-1259, Palo Also, California, 1981.

11. Thomas, P. D., "Numerical Method for Predicting Flow Characteristics and Performance of Nonaxisymmetric Nozzles-Theory," NASA CR 3147, September 1979.

12. Baldwin, B. S. and Lomax, H., "Thin Layer Approximation and Algebraic Model for Separated Turbulent Flow," AIAA Paper 78-257, Huntsville, Alabama, January 1978.

13. Nichols, R. H., "A Two-Equation Model for Compressible Flows, AIAA Paper 90-0494, Reno, Nevada, January 1990.

14. Van Wylen, G. S. and Sonntag, R. E., Fundamentals of Classical Thermodynamics, John Wiley and Sons, Inc., New York, 1973.

15. Anderson, J. D., Jr., Hypersonic and High Temperature Gas Dynamics, McGraw-Hill Book Company, 1989.

16. Gordon and McBride, "Computer Program for Calculation of Complex Chemical Equilibrium Compositions, Rocket Performance Incident and Reflected Shocks and Chapman-Joughet Detonations," NASA SP-273, 1973.

17. Davidson, N., Statistical Mechanics, McGraw-Hill Book Company, New York, 1972.

18. Svehla, R. A., "Thermodynamic and Transport Properties of the Hydrogen-Oxygen System," NASA SP-3011, 1964.

19. Dorrell, E. W., Jr. and Soni, B. K., "IN-GRID: Interactive Two-Dimensional Grid Generation," AEDC-TR-86-49, Arnold Engineering Development Center, Tullahoma, Tennessee, February 1987.

20. Chan, J. S. and Freeman, J. A., "Final Report - Thrust Chamber Performance Using Navier-Stokes Solution," Contract NAS8-35987, MSFC, December 1984.

21. Straub, D., Thermodynamics of Optimized Rocket Propulsions - Extended Lewis Code Fundamentals, Bi Verlag, Basel, Germany, 1989.

22. Stull, D. R., "JANAF Thermochemical Tables; First Addendum," PB 168370-1, Dow Chemical, Midland, Michigan, U. S. Department of Commerce, 1966.

23. Huber, K. P. and Herzberg, G., Molecular Spectra and Molecular Structure, van Nostrand Reinhold Company, New York, 1979.

24. Jaffe, R. L., "The Calculation of High-Temperature Equilibrium and Nonequilibrium Specific Heat Data for N2, O2, and NO," AIAA Paper 87-1633, Honolulu, Hawaii, June 1987.

25. Spectroscopic Data, Vol. I, edited by S. N. Suchard, The Aerospace Corporation, Los Angeles, California.

26. Vincenti, W. G. and Kruger, C. H., Jr., Introduction to Physical Gas Dynamics, Wiley, New York, 1965.

27. Burden, R. L., Faires, J. D., and Reynolds, A. C., Numerical Analysis, Prindle, Weber and Schmidt, Boston, Massachusetts, 1978.

28. Dorrance, W. H., Viscous Hypersonic Flow, McGraw-Hill Book Company, New York, 1962.

29. Armaly, B. F. and Sutton, K., "Viscosity of Multicomponent Partially Ionized Gas Mixtures," AIAA Paper 80-1495, Snowmass, Colorado, July 1980.

30. Armaly, B. F. and Sutton, K., "Thermal Conductivity of Partially Ionized Gas," AIAA Paper 81-1174, Palo Alto, California, June 1981.

31. Hirschfelder, J. O., "Heat Transfer in Chemically Reacting Mixtures. I," The Journal of Chemical Physics, Vol. 26, Part 2, February 1957.

32. Butler, J. N. and Brokaw, R. S., "Thermal Conductivity of Gas Mixtures in Chemical Equilibrium," The Journal of Chemical Physics, Vol. 26, No. 6, June 1957.

APPENDICES

APPENDIX A

PARTITION FUNCTIONS AND SPECTROSCOPIC CONSTANTS

Di-Atomic Molecules

Partition Functions

$$q_{tot,s} = (q_{tr}\, q_{rot}\, q_{vib}\, q_{corr}\, q_{elec})_s$$

$$q_{tr,s} = 0.0256 W^{3/2} T^{5/2}/P$$

$$q_{rot,s} = (\sigma y)^{-1}(1 + y/3 + y^2/15)$$

$$q_{vib,s} = \frac{1 - exp(-u_D)}{1 - exp(-u_v)}, u_D = \theta_D/T,\ u_v = \theta_v/T$$

$$q_{corr,s} = 1 + 2\gamma/y + \delta/(exp(u_c) - 1) + 2X_e u_c/(exp(u_c) - 1) + \frac{y}{3} + \frac{y^2}{15}$$

$$q_{elec,s} = \sum_i g_i\, exp(-\theta_i/T)$$

θ_V, θ_D, θ_i = characteristic temperature for vibration, dissociation and electronic level i, respectively.

Subscript s refers to species s (this subscript has been dropped from the values of $u_{V,s}$, $\theta_{i,s}$, y_s, etc., to simplify the notation above and in the remainder of this appendix, where it is understood that all

values associated with q_s correspond to a single species). γ is a spectroscopic constant not associated with C_p/C_v.

Enthalpy

$$(\overline{H} - \overline{H}^o_O)_{tot} = - \frac{\overline{R}}{(q_{tot}/N)} \frac{\partial(q_{tot}/N)}{\partial(1/T)}\bigg|_P$$

$$(\overline{H} - \overline{H}^o_O)_{tr} = 2.5\, \overline{R}\, T$$

$$(\overline{H} - \overline{H}^o_O)_{rot} = \overline{R}\, T$$

$$(\overline{H} - \overline{H}^o_O)_{vib} = \overline{R}\, T \left[\frac{u_v}{exp\,(u_v) - 1} - \frac{u_D}{exp\,(u_D) - 1} \right]$$

$$(\overline{H} - \overline{H}^o_O)_{corr} = \frac{hc\overline{R}}{k} \left[B_o \left(\frac{2\gamma}{y^2} - \frac{1}{3} \right) + \frac{\omega_o \delta\, exp\,(u_c)}{(exp\,(u_c) - 1)^2} \right]$$

$$(\overline{H} - \overline{H}^o_O)_{elec} = \frac{\overline{R}}{q_{elec}} = \sum_i g_i \theta_i\, exp\,(-\theta_i/T)$$

$$\overline{H}^o_O = \overline{E}^o_O$$

Specific Heat

$$(\overline{C}_{p\,tot} = \left.\frac{\partial \overline{H}}{\partial T}\right|_P = \overline{R}\,T^2 \frac{\partial}{\partial T}\left(\left.\frac{\partial \ell n\,(q_{tot,s}/N)}{\partial T}\right|_P\right)$$

$$\overline{C}_{p\,tr} = 2.5\,\overline{R}$$

$$\overline{C}_{p\,rot} = \overline{R}$$

$$\overline{C}_{p\,vib} = \overline{R}\left[\frac{u_v^2 \exp(u_v)}{(\exp(u_v)-1)^2} - \frac{u_D^2 \exp(u_D)}{(\exp(u_D)-1)^2}\right]$$

$$\overline{C}_{p\,corr} = \overline{R}\left[\frac{4Y}{y} + \frac{\delta u_c^2 \exp(u_c)(\exp(u_c)+1}{(\exp(u_c)-1)^3}\right.$$

$$\left. + \frac{2X u_c^2 \exp(u_c)(4u_c \exp(u_c) - 4\exp(u_c) + 2u_c + 4)}{(\exp(u_c)-1)^4}\right]$$

$$\overline{C}_{p\,elec} = -\frac{\overline{R}}{q_{elec,s}\,T^2}\sum_i g_i \theta_i^2 \exp(-\theta_i) - \frac{\overline{H}_{elec}}{q_{elec}\,T^2}$$

Atoms

Partition Functions

$$q_{tot} = (q_{tr}\, q_{rot}\, q_{vib}\, q_{corr}\, q_{elec})$$

$$q_{tr} = 0.0256 W^{3/2} T^{5/2}/P$$

$$q_{rot} = 1.0$$

$$q_{vib} = 1.0$$

$$q_{corr} = 1.0$$

$$q_{elec} = \sum_i g_i \exp\,(-\theta_i/T)$$

Enthalpy

$$(\overline{H} - \overline{H}^o_O)_{tot} = - \frac{\overline{R}}{(q_{tot}/N)} \frac{\partial(q_{tot}/N)}{\partial(1/T)}\bigg|_P$$

$$(\overline{H} - \overline{H}^o_O)_{tr} = 2.5\, \overline{R}\, T$$

$$(\overline{H} - \overline{H}^o_O)_{rot} = 0.0$$

$$(\overline{H} - \overline{H}^o_O)_{vib} = 0.0$$

$$(\overline{H} - \overline{H}^{o}_{O})_{corr} = 0.0$$

$$(\overline{H} - \overline{H}^{o}_{O})_{elec} = \frac{\overline{R}}{q_{elec,s}} = \sum_{i} g_i \theta_i \exp(-\theta_i/T)$$

Specific Heat

$$(\overline{C}_{p\,tot} = \frac{\partial \overline{H}}{\partial T}\bigg|_{P} = \overline{R}\,T^2 \frac{\partial}{\partial T}\left(\frac{\partial \ell n\,(q_{tot,s}/N)}{\partial T}\bigg|_{P}\right)$$

$$\overline{C}_{p\,tr} = 2.5\,\overline{R}$$

$$\overline{C}_{p\,rot} = 0.0$$

$$\overline{C}_{p\,vib} = 0.0$$

$$\overline{C}_{p\,corr} = 0.0$$

$$\overline{C_{p\,elec}} = -\frac{\overline{R}}{q_{elec}\,T^2} \sum_{i} g_i \theta_i^2 \exp(-\theta_i/T) - \frac{\overline{H}_{elec}}{q_{elec}\,T^2}$$

Tri-Atomic Molecules

Partition Functions

$$q_{tot} = (q_{tr}\, q_{rot}\, q_{vib}\, q_{corr}\, q_{elec})$$

$$q_{tr} = 0.0256 m^{3/2} T^{5/2}/P$$

$$q_{rot} = \frac{6.9358\,(10^{57})}{\sigma}\left(I_x I_y I_z\right)^{1/2} T^{3/2}$$

$$q_{vib} = \prod_i \frac{1}{\left(1 - exp\,(-u_{v_i})\right)}$$

$$q_{corr} = 1.0$$

$$q_{elec} = \sum_i g_i\,(exp\ (-\theta_i/T)$$

Enthalpy

$$(\overline{H} - \overline{H}^o_O)_{tot} = -\frac{\overline{R}}{(q_{tot}/N)} \left.\frac{\partial(q_{tot}/N)}{\partial(1/T)}\right|_P$$

$$(\overline{H} - \overline{H}^o_O)_{tr} = 2.5\ \overline{R}\, T$$

$$(\overline{H} - \overline{H}^o_O)_{rot} = 1.5\ \overline{R}\, T$$

$$(\overline{H} - \overline{H}^o_O)_{vib} = \overline{R}\, T \sum_i \left(\frac{u_{v_i}}{exp\,(u_{v_i}) - 1}\right)$$

$$(\overline{H} - \overline{H}^{o}_{O})_{corr,s} = 0.0$$

$$(\overline{H} - \overline{H}^{o}_{O})_{elec,s} = \frac{\overline{R}}{q_{elec,s}} = \sum_{i} g_i \theta_i \exp(-\theta_i/T)$$

$$\overline{H}^{o}_{O} = \overline{E}^{o}_{O}$$

Specific Heat

$$(\overline{C}_{p\,tot} = \frac{\partial \overline{H}}{\partial T}\bigg|_{P} = \overline{R}\,T^2 \frac{\partial}{\partial T}\left(\frac{\partial \ell n\,(q_{tot}/N)}{\partial T}\bigg|_{P}\right)$$

$$\overline{C}_{p\,tr} = 2.5\,\overline{R}$$

$$\overline{C}_{p\,rot} = 1.5\,\overline{R}$$

$$\overline{C}_{p\,vib} = \overline{R} \sum_{i} \left(\frac{u_{v_i}}{\exp(u_{v_i}}\right)$$

$$\overline{C}_{p\,corr} = 0.0$$

$$\overline{C}_{p\,elec} = -\frac{\overline{R}}{q_{elec}\,T^2} \sum_{i} g_i \theta_i^2 \exp(-\theta_i/T) - \frac{\overline{H}_{elec}}{q_{elec}\,T^2}$$

Spectroscopic Constants

$$u_c = hcw_o/kT = hc(w_e X_e)/kT$$

$$u_v = h\upsilon/kT = hcw_e/kT$$

$$y = B_e hc/kT$$

$$\theta = 1.4388\, T_e\, Kelvin$$

g = Degeneracy

T_e = Characteristic temperature

D_e = Spectroscopic heat of dissociation

w_e = Classical vibrational frequency

X_e = Anharmonicity constant

r_e = Equilibrium separation distance

B_e = Constant relating to moment of inertia, $B_e = h/8\pi^2 I_e c$

α_e = Correction due to changing moment of inertia due to the vibration associated with rotation

I_x, I_y, I_z = Product of moments of inertia

σ = Symmetry number

PHYSICAL CONSTANTS

Speed of light in vacuum, c	2.997925×10^{10} cm/sec
Planck's constant, h	6.6256×10^{-27} erg-sec
Boltzmann's constant, k	1.38054×10^{-16} erg/K
Avogandro's number, $\overline{N}$	6.02252×10^{23}/mole
Universal gas constant, $\overline{R}$	1.9873 cal/(mole-K)

Table A.1 Spectroscopic Constant Data

Species	g	T_e (cm^{-1})	D_e (cm^{-1})	w_e (cm^{-1})	w_eX_e (cm^{-1})	r_e (Å)	B_e (cm^{-1})	α_e (cm^{-1})
Atomic Hydrogen H [22]	1	0						
Atomic Oxygen O [22]	5 3 1 5	0 227.71 326.57 22830.0						
Hydrogen-H_2 [23]	1	0	0.0471	4401.21	121.33	0.74144	60.853	3.062
Oxygen-O_2 [24]	3 2 1 1 6 3 10	0.0 7918.1 13195.1 33057.0 34690.0 35397.8 39279.0	42048.0 34130.0 28852.9 8991.0 7358.0 6651.0 2769.0	1580.19 1483.50 1432.80 794.20 850.00 799.07 200.00	11.98 12.90 14.00 12.73 20.00 12.16	1.2075 1.2156 1.2269 1.5170 1.4800 1.5215 1.9940	1.43768 1.42640 1.40037 0.91500 0.96000 0.91060 0.53000	0.01590 0.01710 0.01820 0.01390 0.02600 0.01410 0
OH [25]	4 2	0 32682.5	$1.88(10^{-3})$ $2.04(10^{-3})$	3735.21 3184.28	82.81 97.84	0.9706 1.0121	18.871 17.355	0.714 0.867
H_2O $\sigma = 2$* [22]	1 1 1	0 0 0		3657.05 1594.59 3755.79				
HO_2 $\sigma = 1$** [22]	1 1 1	0 0 0		1389.4 1101 3414				

* $\sqrt{I_x I_y I_z} = 2.4012\,(10^{-60})$

** $\sqrt{I_x I_y I_z} = 2.535\,(10^{-59})$

APPENDIX B

EQUILIBRIUM CONSTANTS [26]

For the chemical reaction

$$\nu_A A + \nu_B B \leftrightarrows \nu_C C + \nu_D D$$

The equilibrium constant

$$K = \prod_i q_{tot_i}^{\nu_i} \exp(-\Delta \overline{H} / \overline{R} T)$$

where i is each species in the reaction,

ν_i is positive for the products and negative for the reactants,

ΔH is the heat of reaction.

APPENDIX C

EQUILIBRIUM COMPOSITION NEWTON-RAPHSON EQUATIONS

Definition of Equilibrium Constant

1) $$K_1' = \frac{[X_H]^2}{[X_{H_2}]}$$

2) $$K_2' = \frac{[X_o]^2}{[X_{O_2}]}$$

3) $$K_3' = \frac{[X_o][X_H]}{[X_{OH}]}$$

4) $$K_4' = \frac{[X_H]^2[X_O]}{[X_{H_2O}]}$$

5) $$K_5' = \frac{[X_H][X_O]^2}{[X_{HO_2}]}$$

7 unknowns, need 2 more equations

Sum of Mole Fractions

6) $$X_H + X_O + X_{H_2} + X_{O_2} + X_{OH} + X_{H_2O} + X_{HO_2} = 1$$

Continuity

$$aH_2 + bO_2 \rightarrow cH + dO + eH_2 + fO_2 + hOH + iH_2O + jHO_2$$

7) $$2b = d + 2f + h + i + 2j$$

8) $$2a = c + 2e + h + 2i + j$$

Let f = oxygen to fuel weight ratio, then

$$f = \frac{b(31.9988)}{a(2.016)}$$

Taking a = 1 gives

$$b = \frac{2.016}{31.9988} f = .063f$$

so Equations (7) and (8) can be written as

9) $$2 = c + 2e + h + 2i + j$$

10) $$2(.063f) = d + 2f + h + e + 2j$$

Dividing Equations (9) and (10) by total number of moles η_T, gives

11) $$C_2 = \frac{2}{\eta_T} = X_H + 2\left[X_{H_2}\right] + X_{OH} + 2\left[X_{H_2O}\right] + X_{HO_2}$$

12) $$C_1 = \frac{2(.063)f}{\eta_T} = \frac{.126f}{\eta_T} = X_O + 2\left[X_{O_2}\right] + X_{OH} + 2\left[X_{HO_2}\right] + X_{H_2O}$$

Solving for η_T gives

13) $$\frac{2}{C_2} = \frac{.126\, f}{C_1} = \eta_T .$$

The Newton-Raphson method is used to solve the set of seven non-linear algebraic equations. If the equations are of the form

$$F(X) = \begin{bmatrix} f1\ (X_1, X_2, X_3, \ldots X_i) \\ f2\ (X_1, X_2, X_3, \ldots X_i) \\ \vdots \\ fi\ (X_1, X_2, X_3, \ldots X_i) \end{bmatrix} = 0$$

they can be solved for X by the equation

$$X^N = X^{N-1} - J(X^{N-1})^{-1} F(X^{N-1})$$

where N is the iteration number and J(X)-1 is the inverse of the Jacobian matrix

$$J(x) = \begin{bmatrix} \frac{\partial f1(x)}{\partial x1} & \frac{\partial f1(x)}{\partial x2} & \cdots & \frac{\partial f1(x)}{\partial x_n} \\ \frac{\partial f2(x)}{\partial x1} & \frac{\partial f2(x)}{\partial x2} & \cdots & \frac{\partial f2(x)}{\partial x_n} \\ \frac{\partial fn(x)}{\partial x1} & \frac{\partial fn(x)}{\partial x2} & \cdots & \frac{\partial fn(x)}{\partial x_n} \end{bmatrix}, \qquad [27].$$

Setting the seven equations equal to zero gives

$$f_1 = \left[X_H\right]^2 - K_1' \left[X_{H_2}\right] = 0$$

$$f_2 = \left[X_O\right]^2 - K_2' \left[X_{O_2}\right] = 0$$

$$f_3 = \left[X_H\right]\left[X_O\right] - K_3' \left[X_{OH}\right] = 0$$

$$f_4 = \left[X_H\right]^2\left[X_O\right] - K_4' \left[X_{H_2O}\right] = 0$$

$$f_5 = \left[X_H\right]\left[X_O\right]^2 - K_5' \left[X_{HO_2}\right] = 0$$

$$f_6 = X_H + X_O + X_{H_2} + X_{O_2} + X_{OH} + X_{H_2O} + X_{HO_2} - 1 = 0$$

$$f_7 = \frac{C_1}{.126\,f} - \frac{C_2}{2} = 0$$

Filling the Jacobian Matrix. we have

$$
\begin{bmatrix}
2[X_H] & 0 & -K_1' & 0 & 0 & 0 & 0 \\
0 & 2[X_O] & 0 & -K_2' & 0 & 0 & 0 \\
H_O & X_H & 0 & 0 & -K_3' & 0 & 0 \\
2[X_H][X_O] & [X_H]^2 & 0 & 0 & 0 & -K_4' & 0 \\
[X_O]^2 & 2[X_H][X_O] & 0 & 0 & 0 & 0 & -K_5' \\
1 & 1 & 1 & 1 & 1 & 1 & 1 \\
\frac{1}{2} & \frac{1}{.126f} & -1 & \frac{2}{.126f} & & \frac{1}{.126f} & -\frac{1}{2}
\end{bmatrix}
$$

APPENDIX D

PARTIAL DERIVATIVE OF THE EQUILIBRIUM CONSTANT

$\dot{K}_j = \frac{\partial K'}{\partial T}$ *for constant pressure and for constant volume.*

Constant Pressure $\dot{K}_j$

Start with van Hoff Equation

$$\frac{d\,\ell n\,K}{dT} = \frac{\Delta H^o}{\overline{R}\,T^2}$$

$$\dot{K}_j = \frac{dK}{dT} = \frac{\Delta H^o K}{\overline{R}\,T^2}$$

Substitute

$$K_j = K'\left(\frac{P}{P^o}\right)^{\Sigma v_i}$$

$$\frac{dK'\left(\frac{P}{P_o}\right)^{\Sigma v_i}}{dT} = \frac{\Delta H^o K'\left(\frac{P}{P_o}\right)^{\Sigma v_i}}{\overline{R}\,T^2}$$

For Constant Pressure

$$\left(\frac{P}{P_o}\right)^{\Sigma v_i}\frac{\partial K'}{\partial T}\bigg|_P = \frac{\Delta H^o K'\left(\frac{P}{P_o}\right)^{\Sigma v_i}}{\overline{R}\,T^2}$$

$$\boxed{\dot{K}_j = \frac{\partial K'}{\partial T}\bigg|_P = \frac{\Delta H^o K'}{\overline{R}\,T^2}}$$

Kj' for Constant Density

As before

$$\frac{dK'\left(\frac{P}{P_o}\right)^{\Sigma v_i}}{dT} = \frac{\Delta H^o K'\left(\frac{P}{P_o}\right)^{\Sigma v_i}}{\overline{R}\,T^2}$$

Chain Rule

$$\left(\frac{P}{P_o}\right)^{\Sigma v x_i}\frac{dK'}{dT} + K'\frac{d\left[\left(\frac{P}{P_o}\right)^{\Sigma v_i}\right]}{dT} = \left(\frac{P}{P_o}\right)^{\Sigma v x_i}\frac{dK'}{dT} + K'\sum v_i\left(\frac{P}{P_o}\right)^{\Sigma v_i - 1}\frac{dP}{dT}\left(\frac{1}{P_o}\right)$$

$$= \frac{\Delta H^o K'\left(\frac{P}{P_o}\right)^{\Sigma v_i}}{\overline{R}\,T^2}$$

Perfect Gas

$$P = \rho RT$$

$$\left.\frac{\partial P}{\partial T}\right|_{\rho} = \rho R = \frac{P}{RT}R$$

Substitute and Solve for

$$\dot{K}' = \left.\frac{\partial K'}{\partial T}\right|_{\rho}$$

$$\left(\frac{P}{P_o}\right)^{\Sigma v_i}\frac{dK'}{dT} + K\sum v_i\left(\frac{P}{P_o}\right)^{\Sigma v_i - 1}\left(\frac{1}{P_o}\right)\frac{P}{T} = \frac{\Delta H K'\left(\frac{P}{P_o}\right)^{\Sigma v_i}}{\overline{R}\,T^2}$$

$$\left(\frac{P}{P_o}\right)^{\Sigma v_i}\frac{dK'}{dT}\Big)_\rho = \frac{\Delta H K'\left(\frac{P}{P_o}\right)^{\Sigma v_i}}{\overline{R}\,T^2} - K'\sum v_i\left(\frac{P}{P_o}\right)^{\Sigma v_i - 1}\frac{P}{T}\,\frac{1}{P_o}$$

$$\frac{\partial K'}{\partial T}\Big)_\rho = \frac{\Delta H^o K'}{\overline{R}\,T^2} - \frac{K'\sum v_i\,\frac{P}{T}\,\frac{1}{P_o}}{\left(\frac{P}{P_o}\right)}$$

$$\left.\frac{\partial K'}{\partial T}\right|_\rho = K'\left[\frac{\Delta H^o}{\overline{R}\,T^2} - \frac{\sum v_i}{T}\right].$$

APPENDIX E

SUMMARY OF TRANSPORT PROPERTY EQUATIONS

$\sigma^2\Omega(2,2)^*$ = collision integral for viscosity
$\sigma^2\Omega(1,1)^*$ = collision integral for diffusion

I. Viscosity

(a)
$$\mu_i = 266.93 \times 10^{-7} \frac{\sqrt{W_i T}}{\sigma^2 \Omega^{(2,2)^*}} \frac{q}{cm-sec}$$

(Dorrance [28])

(b)
$$\mu_{mix} = \sum_{k,k\neq i} \frac{2X_i X_k}{\mu_{ik}} \frac{W_i W_k}{(W_i + W_k)^2} \left(\frac{5}{3} A^*_{ik} + \frac{m_k}{m_i} \right)$$

(Armaly and Sutton [29])

where
$$\mu_{ij} = \left(\frac{32\, W_i W_j}{W_i W_j} \right)^{1/2} \Big/ \left(\frac{W_i^{1/4}}{\mu_i^{1/2}} F_{ij} \frac{W_j^{1/4}}{\mu_j^{1/2}} B_{ij} \right)^{12}$$

and
$$F_{ij} = \left(\frac{\Omega_{ij}^{(2,2)^*}}{\Omega_{ii}^{(2,2)^*}} \right)^{1/2} = 1,$$

$$A^*_{ij} = \frac{\Omega_{ij}^{(2,2)^*}}{\Omega_{ij}^{(1,1)^*}}, \qquad B_{ij} = \left(\frac{\Omega_{ij}^{(2,2)^*}}{\Omega_{jj}^{(2,2)^*}} \right)^{1/2}$$

II. Thermal Conductivity

(a)
$$k_{i_{tr}} = \frac{15}{4} \frac{\overline{R}}{W_i} \mu_i \frac{cal}{cm - sec - K}$$

(Dorrance [28])

(b)

$$k_{mix,tr} = \frac{15}{4}\,\bar{R} \sum_{k,k=i} \frac{X_k}{\mu_{ik}} \frac{W_i W_k}{(W_i + W_k)^3} \frac{\frac{15}{2} W_i^2 + \frac{5}{2} W_k^2 + 4 W_i W_k A_{ik}^*}{A_{ik}^*}$$

Armaly and Sutton [30])

(c)

$$k_{mix,tr} = \sum_i \frac{X_i W_i \left(\frac{\bar{C}_{pi}}{\bar{R}} - \frac{5}{2} \right)}{\sum_j X_j \frac{W_i W_j}{W_i + W_j} \sigma_{ij} \Omega^{(2,2)*}} \frac{P}{\bar{R} T} D_{ij}$$

(Hirschfelder[31])

(d)

$$k_{mix,reac} = \frac{1}{RT^2} \begin{vmatrix} 0 & \Delta H_1 & \cdots & \Delta H_q \\ \Delta H_1 & A_{11} & \cdots & A_{1q} \\ \vdots & \vdots & & \vdots \\ \Delta H_q & A_{q1} & \cdots & A_{qq} \end{vmatrix} \Bigg/ \begin{vmatrix} A_{11} & \cdots & A_{1q} \\ \vdots & & \vdots \\ A_{q1} & \cdots & A_{qq} \end{vmatrix}$$

(Butler and Brokaw [32])

with

$$\Delta H = \sum_{i=1}^{s} \upsilon_i (\Delta H_{fo}^o)_i$$

and

$$A_{ij} = A_{ji} = \sum_{k=1}^{s-1} \sum_{l=k+1}^{x} \left(\frac{RT}{\overline{D}_{kl\,p}} \right) X_k X_l$$

$$x \left[\frac{v_{ik}}{X_k} - \frac{v_{il}}{X_l} \right] \left[\frac{v_{jk}}{X_k} - \frac{v_{jl}}{X_l} \right], i,j = 1,2,\ldots s \,(number\ of\ species$$

$$k_{tot,mix} = (k_{tr} + k_{int} + k_{reac})_{mix}$$

III. Binary Diffusion Coefficient

$$\overline{D}_{ij} = \overline{D}_{ji} = 262.8\left(10^{-5}\right) \left[T^3 \frac{W_i + W_j}{2W_i W_j} \right]^{1/2} / p\sigma_{ij}^2 \Omega^{(1,1)^*} \frac{cm^2}{sec}$$

(Dorrance [28]).

APPENDIX F

METHOD OF BISECTION

The method of bisection is an iterative method for finding an approximate solution (P) to a continuous function of the form $f(x) = 0$ on the interval [a,b] where $f(a)$ and $f(b)$ have opposite signs.

The method calls for a repeated halving of subintervals of [a,b] and at each step locating the "half" containing P. The bisection algorithm is as follows:

To find a solution to $f(x) = 0$ given the continuous function f on the interval [a,b] where $f(a)$ and $f(b)$ have opposite signs:

INPUT endpoints a, b; tolerance TOL; maximum number of iterations N_O.

OUTPUT approximate solution p or message of failure.

Step 1 Set i = 1.

Step 2 While $i \leq N_O$ do Steps 3-6.

Step 3 Set p = a + (b-a)/2. (Compute p_i.)

Step 4 If $f(p) = 0$ or $(b-a)/2 < TOL$ then

OUTPUT (p); (Procedure completed successfully.)

STOP.

Step 5 Set i = i + 1.

Step 6 If $f(a)f(p) > 0$ then set a = p (Compute a_i, b_i.)

Step 7 OUTPUT ('Method failed after N_O iterations, N_O = ', N_O);

(Procedure completed unsuccessfully.)

STOP.

Burden and Faires [27].

APPENDIX G

EQUATIONS FOR NONDIMENSIONALIZATION OF PARC

The subscript d refers to dimensional properties. The subscript ref refers to reference properties. From the original PARC code [5].

Lengths	$X = X_d/X_{ref}$
Densities	$\rho = \rho_d/\rho_{ref}$
Velocities	$U = U_d/a_{ref}$
Temperatures	$T = T_d/T_{ref}$
Pressures	$P = P_d/\gamma P_{ref}$
Total energies	$E = E_d/\gamma P_{ref}$
Reynolds number	$Re = \rho_{ref} a_{ref} X_{ref}/\mu_{ref}$

For the equilibrium upgrade

Compressibility Factor

$$Z = \frac{\frac{W_d}{W_{ref}}}{\gamma_{ref}} \qquad W = Molecular\ Weight$$

Speed of Sound

$$a = \frac{a_d}{\sqrt{\gamma_{ref} R T_{ref}}}$$

Constant Pressure Specific Heat

$$C_p = \frac{C_{p_d}}{\left(\gamma_{ref} - 1\right) C_{p_{ref}}}$$

Speed of sound at reference state is given by

$$a_{ref} = \frac{\gamma_{ref} P_{ref}}{\rho_{ref}} .$$

VITA

Brian Lee Myruski was born in Fairfax, Virginia on December 14, 1964. He graduated from Stafford High School in Fredericksburg, Virginia in 1983. He entered the University of Tennessee in Knoxville in the fall of 1983 on an Athletic Scholarship with the Varsity Swim Team. During his tenure with the swim team he was named All-American and Academic All-American. He graduated from the University of Tennessee in 1988 with a Bachelor of Science, Mechanical Engineering degree. He entered the University of Tennessee Space Institute in August 1988 where he accepted a graduate research assistantship with the Center for Advanced Space Propulsion (CASP). In August 1990, Brian completed his studies at the Space Institute and received a Master of Science degree in Mechanical Engineering.